System-Level Optimization Approach for Small Satellite Moon Missions by Using Electric Propulsion and Mission Cost Survey for Turkish Space Economy

by

Ozan Kara

A Dissertation Submitted to the
Graduate School of Sciences and Engineering
in Partial Fulfillment of the Requirements for
the Degree of

Master of Science

in

Department of Mechanical Engineering

KOÇ
UNIVERSITY

January 26, 2016

System-Level Optimization Approach for Small Satellite Moon Missions by Using Electric Propulsion and Mission Cost Survey for Turkish Space Economy

Koç University

Graduate School of Sciences and Engineering

This is to certify that I have examined this copy of a master's thesis by

Ozan Kara

and have found that it is complete and satisfactory in all respects,
and that any and all revisions required by the final
examining committee have been made.

Committee Members:

_____

Assist. Prof. Arif Karabeyoğlu

_____

Assoc. Prof. Metin Muradoğlu

_____

Assoc. Prof. Onur Tunçer

Date: _____

to my family, to space community

ABSTRACT

This thesis presents a system-level optimization approach to perform low-cost small satellite lunar mission by using existing ion and hall propulsion systems. The system-level optimization finds minimum flight time accompanied with maximum payload mass, minimum initial spacecraft mass and optimum spacecraft volume values. To create accurate mission analysis two types of optimization approaches are studied; iterative method and constrained optimization method. These methods calculates various mission scenarios such as ion thruster LEO departure orbit, ion thruster GEO departure orbit and hall thruster LEO and GEO departure orbits. In the iterative method, ion thruster LEO departure case results a spacecraft mass of 213 kg and corresponding 23mN thrust value. This case needs 64 kg xenon propellant to perform 980 days flight duration to the Moon. The optimum spacecraft volume is found as $0.70m^3$ and costs \$108.5M. Same thrust level of 23mN for GEO departure case takes 880 days with 58 kg xenon gas. The total cost reduces \$2.5M. However by using hall thruster system, LEO departure case needs $0.8m^3$, 247 kg spacecraft including 82 kg xenon propellant. 77 mN thrust results 208 days flight time towards the Moon that ends up with \$121M total cost. The GEO departure Hall case reduces the flight time an amount of 45 days by consuming 65 kg propellant. Total spacecraft mass and volume values are 230 kg, $0.71m^3$ that costs \$115M. Finally, the overall cost of lunar mission cases is discussed for Turkey space economy. The space technology demand of investment will increase up to \$400M in 2020s, an overall cost with \$100M lunar mission seems applicable however needs significant collaboration among universities, private sector and government.

ÖZETÇE

Bu çalışma iyon ve hall itki sistemlerini kullanarak, düşük maliyetli küçük uydu Ay görevi oluşturmak için sistem seviyesinde bir eniyileme yaklaşımı sunmaktadır. Sistem seviyesindeki eniyileme, maksimum faydalı yük kütlesi, uzay aracı minimum ilk kütlesi ve ideal uzay aracı hacim değerleri ile birlikte minimum uçuş zamanını bulmaktadır. Kesin bir görev analizi için iki tip eniyileme yaklaşımı çalışılmıştır; yinelemeli metot ve kısıtlı eniyileme metodu. Bu metotlar, iyon itki sistemi ile alçak yörüngeden (LEO) fırlatılan, iyon itki sistemi ile jeostatik yörüngeden (GEO) fırlatılan, hall itki sistemi ile alçak yörüngeden (LEO) fırlatılan ve hall itki sistemi ile jeostatik yörüngeden (GEO) fırlatılan, gibi çeşitli görev senaryoları hesaplamaktadırlar. Yinelemeli metotta, iyon itki sistemi ile alçak yörüngeden fırlatılan durum için uzay aracı kütlesi 213 kg ve itki sistemi değeri ise 23mN olmaktadır. Bu durum 980 günlük uçuş süresini oluşturmak için 64 kg ksenon yakıtı gerektiriyor. İdeal uzay aracı hacmi $0.70m^3$ olarak bulunur ve \$108M maliyetlidir. Aynı itki seviyesi olan 23mN ile jeostatik yörüngeden fırlatılan durum ise 880 günlük uçuş zamanı ve 58 kg ksenon yakıtı gerektirmektedir. Bu durumda, toplam maliyet \$2.5M azalmaktadır. Bunun yanında, hall itki sistemi kullanılarak gerçekleştirilen alçak yörünge görev senaryosu $0.8m^3$ uzay aracı hacmi, 287 kg uzay aracı ilk kütlesi ve 82 kg ksenon yakıtı gerektirmektedir. 77mN'luk itki sistemi, Ay'a doğru 208 günlük uçuş zamanı gerektirir ve \$121M bir maliyeti vardır. Jeostatik yörünge fırlatmalı Hall durumu toplam uçuş zamanını 65 kg ksenon yakıtı kullanarak 45 gün azaltır. Toplam uzay aracı kütlesi 230 kg, uzay aracı hacmi $0.71m^3$ ve maliyeti \$115M olarak bulunur. Son olarak Ay görevi ortalama maliyeti Türkiye uzay ekonomisi için tartışılmıştır. Uzay teknoloji talep yatırımları 2020'lerde \$400M'a kadar artacaktır. \$100M'lık bir ay görevi uygulanabilir görünse de üniversiteler, özel sektör ve devlet arasında çok önemli işbirliği gerektirmektedir.

ACKNOWLEDGMENTS

First and foremost, I am greatly indebted to my family members; my father Ekrem Kara, my mother Songül Kara, my precious sister Damlanur Kara and my uncle like my second dad Erdoğan Kara. Their unconditional supports and encouragements helped me to go through this space journey. Thank you for everything!

I gratefully acknowledge the many supports of my advisor Arif Karabeyoğlu during my master study at KOC University.

I would also like to express my sincere gratitude to my colleague Hadi Nozari. We had great memories while discussing academic life and looking for a new car from Ayvalık! With his friendship I did not feel alone and found always a supportive person. He is always casting his bread upon the waters!

I would also like to thank my friends Elena Toson and Samir Donmazov for their supports during my studies.

I would like to share my special thanks to my friends Çağrı Kılıç and Emel Şen Kılıç. They have always been first people I share my devotion to space. Thank you Emel for helping me to understand drug design course! Also, Thank you Çağrı for your supports related to Turkish Space Economy section of this thesis.

I am so thankful to have very good friends in my life. First, I would like to thank Bilgehan Özcan, the man who always plays Magic the gathering! He is my friend since 2008 and will always my best friend in my life with Seinfield quotes. Another great friend Hüseyin Fırat Güldür, thank you for sharing ITU Gölet dormitory memories and project ideas with me.

Special thanks for my lovely friend Pelin Peker, I will never forget your kind and precious supports.

TABLE OF CONTENTS

LIST OF TABLES

LIST OF FIGURES

NOMENCLATURE

A_{sa} = Solar Array Area, m^2

I_d = Inherent Degradation

I_{sp} = Specific Impulse of Thruster, seconds

M = Molar Mass of the gas, g/mol

$M_{battery}$= Battery Mass, kg

M_{dry}= Dry Mass, includes all subsystems excludes propellant mass, kg

$M_{propellant}$= Propellant Mass, kg

$M_{payload}$= Payload Mass kg

M_{sa}= Solar Array Mass kg

$M_{subtotal}$= Subtotal Mass, excludes solar array, battery, propellant tank and propellant masses, kg

M_{th} = Thruster Mass, kg

M_{thppu} = Thruster Power Processing Unit Mass, kg

M_{total}=Total (Initial) Spacecraft Mass, kg

M_{tank}= Propellant Tank Mass, kg

P = Propellant Storage Tank Pressure, MPa

P_0 = Solar Cell Power per meter square, W/m^2

P_{th}= Thruster Power, Watt

$P_{payload}$= Payload Power, Watt

R = Ideal Gas Constant, J/Kmol

$R_{0,f}$ = Initial and Final Orbital Altitudes, km

T = Thrust, mN and Storage Tank Temperature, Kelvin

t_{flight} = Spacecraft Flight Time or Burn Time, days or years

$V_{0,f}$ = Initial and Final Orbital Velocities, km/s

V_{SC} = Spacecraft Volume, m^3

V_{tank} = Propellant Tank Volume, m^3

β_0 = Initial Thrust yaw angle, degree

θ = Solar Incidence angle, degree

Δi = Orbital Inclination Change, radians

ρ_{tank} = Tank Density kg/m^3

$\rho_{propellant}$ = Propellant Density, kg/m^3

$\sigma_{yieldstrength}$ = Yield Strength of the Propellant Tank, Pa

μ_{th} = Thruster efficiency, percentage

Chapter 1

INTRODUCTION

The Moon has been one of the engrossing bodies to observe fundamental changes in space environment. The Moon with the tenuous atmosphere allows energetic particles leaping up and falling back to the surface. Also, observations of the tiny particle movement, lunar soil and dust atmosphere explains magnetic interactions in near and far sides [1]. The researches had conducted various missions such as SMART-1, Hayabusa, Clementine, Lunar Prospector and LADEE gathered data and images about radiation impacts, volcanic activities and water/ice conditions on the Moon surface. After these fundamental efforts, the next path for Moon exploration should be standardization of low-cost small spacecraft can be managed by universities. Therefore, I seek to develop a system-level optimization process for small satellite standardization for low cost Moon operations which universities, governments and companies can easily perform.

Potential microsatellite missions with onboard propulsion system have been studied by many researchers. The European Student Moon Orbiter (ESMO) mission was a science mission concept designed by ESA to be launched into GTO with onboard liquid bi-propellant [2]. ESMO is 250 kg and includes secondary 6kg nanosatellite for lunar gravity mapping. A similar research was conducted by NASA which involved the American Student Moon Orbiter (ASMO). ASMO is 180 kg satellite that is conceived to accommodate a 10 kg payload in a highly elliptical lunar orbit. ASMO uses cold gas thrusters and also ATK STAR type solid motor [3]. An overarching study by Pergola presents a 100 kg, 1140W satellite design for asteroid Cruithne including indirect optimization trajectory design and detail spacecraft layout [4]. Pergola

estimates xenon ion propulsion with 35 kg propellant. These concepts did not have accurate cost analysis by using the system-level optimization. In addition, these mission concepts considered only one type of trajectory transfer case that is needed to be improved for the detail mission analysis.

The objective of this thesis to find reliable system-level optimization approach for small satellite lunar missions by using ion and hall thrusters. Unlike previous concept designs, this study uses real historical data of thrusters and small spacecraft mission, compares performances of ion and hall engines and includes detail cost analysis. The inspected mission scenario is considered where the target is the Moon by means of low-thrust, time-optimal circle-to-circle non-coplanar transfer. I perform LEO and GEO departure cases to observe discernible outcomes of ΔV requirements, propellant consumptions and the total cost. In addition, I calculate optimum propellant density, pressure and tankage fractions. Eclipse time is also significant driver to calculate spacecraft battery mass. To compare various optimization methods, I estimated both an iterative optimization process and a constrained optimization process by using MATLAB. The main functions of optimization routines comes from best fit equations obtained from 12 ion engines, 12 hall engines and 15 small satellites all flew to the Moon, comets and asteroids. Therefore, the system-level optimization gives minimum flight time and corresponding spacecraft mass, payload mass, propellant mass, spacecraft volume, propellant tank volume, solar array area, total required power and total mission cost for a potential small satellite Moon mission.

Another objective of the thesis is the assessment system-level optimization for Turkish Space Industry. Turkey is in the stage of developing, producing and operating communication satellites, Earth observation satellites and scientific CubeSat itself. The space road map of Turkey describes that a variety of spacecraft systems shall be tested for upcoming space studies. In order to estimate the needs of satisfied future missions and show the benefits of small satellites, an interplanetary mission would be the next step to keep pace with the rapidly developing area of satellite technology.

The cost analysis of the system-level optimization of small satellite moon mission

case is discussed within the Turkey Export Strategy and Action Plan. Due to the space technology demand of investment that will reach $400M by 2023 [5], a $100M lunar mission cost including launch, operation and development might be accessible goal for Turkey.

Chapter 2

ELECTRIC PROPULSION REVIEW

This chapter introduces the technical background of electric propulsion systems. Among types of electric propulsion systems, ion and hall thrusters are the most conventional ones. In this chapter I specify the selected ion and hall thrusters for system-level optimization of small satellite Moon missions. By using selected thrusters, I apply curve fitting methodology to understand the relation among thrust level, specific impulse, thruster input power and thruster efficiency. Curve fitting equations are directly used in optimization processes in order to determine mission parameters such as flight duration, initial spacecraft mass, spacecraft volume and the total mission cost.

2.1 Types of Electric Propulsion Systems

Electric propulsion operates with an independent energy source in order to increase propellant exhaust velocity. However in chemical propulsion, combustion process heats the propellant itself and ejects that supersonic velocity through a nozzle. The performance of the electric propulsion systems is determined by following parameters; thrust, specific impulse, efficiency and thruster power. Electric propulsion systems provides high specific impulse and high thruster input power compared with chemical propulsion systems. Therefore the thermal heating is one consideration that effects spacecraft insulation system and architecture design.

The types of thrusters are classified as electrothermal, electrostatic, or electromagnetic. Electrothermal thruster uses resistance or arcjet in order to heat the propellant up and expand through the nozzle. Electromagnetic thruster type mainly operates with the combination of electric and magnetic fields to create thrust with hot propel-

lant gasses [6]. Finally mostly conventional electric propulsion type is electrostatic thrusters ionizes neutral propellant gas with magnetic fields and electric fields.

The Table 2.1 illustrates electric propulsion systems including their specific impulse, input power, efficiency range and propellant types. Especially ion and hall thrusters are mostly used in space industry. Deep Space 1, Hayabusa and Smart-1 missions, NSTAR and XIPS engines are main examples that all used electric propulsion systems [7, 8, 9]. Ion and Hall thrusters use heavy inert gas such as argon and xenon. As Goebel stated [10] xenon is more preferable which is not hazardous, does not condense on spacecraft components that are above cryogenic temperatures, creates higher thrust for a given input power and easily stored at high densities and low tank mass fractions.

Table 2.1: Electric propulsion thrusters parameters [11]

Thruster	Propellant	Specific Impulse (seconds)	Input Power (watts)	Efficiency (%)
Resistojet	N_2H_4 monopropellant	300	500-1000	65-90
Arcjet	N_2H_4 monopropellant	500-600	900-2200	25-45
PPTs	Teflon	850-1200	< 200	7-13
Ion	Xenon/Argon	2500-3600	400-4300	40-80
Hall	Xenon/Argon	1500-2000	1500-4500	35-60

The Table 2.1 shows that ion and hall thrusters have higher specific impulse, input power and efficiency range compared to other conventional electric propulsion systems. Therefore the scope of the system-level optimization is to use only ion and hall thrusters.

2.2 Curve Fitting Methodology

The structure of the system-level optimization process contains specifications of selected ion and hall thruster models. First, most of the real world thrusters is analyzed

as [12] did in his research. Best fit equations is applied to the thruster system parameters and curve fittings are obtained due to thrust versus specific impulse, thrust versus efficiency, thrust versus thruster mass and thrust versus thruster input power. Therefore the best fit equations is used in the system-level equations to predict mission and spacecraft parameters such as spacecraft mass, volume, cost, propellant mass, tank and the mission flight time. Unlike Chiasson who considered 385 specific thrusters, I only analyzed 12 ion thrusters and 12 hall thrusters. The thruster input power and thruster mass are main reasons narrowing down the thruster selection for small satellite Moon mission design. Table 2.2 and Table 2.3 present the list of selected ion and hall thrusters. Ion and hall thruster data relations shows high regression rates in curve fitting. Therefore best fit equations are used into the main algorithm of the iterative optimization method.

Another important parameter which is required for the system-level optimization is the thruster power procession unit (PPU) mass. From the Table 2.4, best fit equation is formed by thrust versus PPU mass relation is substituted into the iterative method. Table 2.4 shows high regression rate that increase in thrust level requires bigger and heavier power procession units for the spacecraft thrusters.

2.3 Selected Ion Thrusters

Ion engines uses potential difference between screen and accelerator grids in order to accelerate ionized propellant. The positively charged grid called as screen grid and negatively charged grid called as accelerator grid. Ionization of the propellant gas is performed by electron bombardment in the cathode chamber. The neutral atoms of propellant gas such as xenon collides with negative charges in the chamber therefore positively charged atoms are released from the propellant gas. Released ions pass through an electrical field created by two grids in order to create a thrust.

In this research xenon propellant ion engines have been considered using Table 2.2. The best fit equations of the Table 2.2 can be found in Figure A.1 to A.4. The regression rates of the figures ranging between 0.7 and 0.98 provide accurate

modelling.

Table 2.2: ION thruster data used for system-level optimization process [12]

Thruster Name	$T(mN)$	$M_{th}(kg)$	$I_{sp}(s)$	$P_{th}(W)$	$\mu_{th}(\%)$
n10	8.1	1.3	2910	340	36
Eureca	10	1.5	3300	440	36.8
RMT	12	2	3600	480	55
RIT-10	15	1	3058	459	36
ARTEMIS	15	1.6	3000	600	37.7
KRC	19	2	3500	494	65
ETS6	23.3	3.7	2910	600	55.43
RIT-25	25	1.7	3060	800	67
DERA T5	25	1.7	3110	644	60
JPL	31	2.5	3200	900	66
RIT-10 EVO	41	1.8	3300	1050	67
RIT15	50	1.9	3600	1350	67

2.4 Selected Hall Effect Thrusters

Apart from ion engines, hall thrusters use the combination of electric and magnetic fields in order to accelerate ionized propellant. The propellant gas is injected into a thruster chamber. There are magnets, an anode and a cathode inside the thruster chamber. Magnets creates magnetic field and an anode and cathode system create an axial electric field through the exit of the chamber. Therefore the axial electric field accelerate ions from cathode towards the thruster exit. Again the xenon is the preferable gas due to its molecular mass, low ionization potential and easy to handle [12].

Existing hall thrusters with thrust values between 13 and 300 mN are investigated for this research. Best fit equations of the Table 2.3 can be found in Figure A.4 to

A.8. The regression rates of the figures ranging between 0.7 and 0.98. Due to the high regression rates best fittings provide accurate results for optimization process.

Table 2.3: HALL thruster data used for system-level optimization process [12]

Thruster Name	$T(mN)$	$M_{th}(kg)$	$I_{sp}(s)$	$P_{th}(W)$	$\mu_{th}(\%)$
Moskow SPT-30	13	0.4	1170	260	30
BHT-200	17	1.1	1390	300	32.5
BHT-600	17	0.9	1600	600	45
SPT-50	20	0.9	1100	350	35
BHT-HD600	36	2.2	1700	600	50
SPT-70	40	2	1500	700	45
BHT-HD1000	55.5	3.5	1700	1000	56
D35	82	4.4	1263	1230	40
PPS 1350G	90	4.5	1650	1500	45
SPT-100	100	3.5	1600	1400	50
Thales HEMP	152	6	3500	3000	58
DS-HET	300	12	3000	5000	50

2.5 Thruster Power Processing Unit Mass Analysis

Another parameter in order to consider within the optimization processes is the thruster power processing unit (PPU) mass distribution. Thruster PPU mass increases as engine thrust increases. Because high thrust values needs more thruster power that means heavier thruster PPUs. Therefore best fit analysis for thrust versus thruster PPU is presented in Table 2.4.

The Table 2.4 shows proportional distribution of PPU mass with respect to engine thrust values. This distribution provides accurate best fitting equations for optimization processes.

Table 2.4: Selected Thrusters: Thrust versus Power Processing Unit Mass

Thruster Name	$T(mN)$	$M_{thppu}(kg)$
DASA [13]	15	9.3
RITA - 10 Artemis [14]	15	8.8
MEPS - 300W PPU [15]	15	7
XIPS 13 [16]	17.8	6.8
Hughes [13]	17.8	6.8
ALTA HT-100D [15]	18	7
T5 - ESA GOCE [17]	20	17
PPS – 1350 [18]	90	10.4
NSTAR [19]	92	15
SPT – 100 [20]	100	10.4
T6 – Qinetiq [21]	143	38
MELCO [22]	200	26.4
NEXT [23]	238	37.6
HiPEP [23]	440	50
Nexis [23]	470	4.2

Chapter 3

SMALL SPACECRAFT MOON AND DEEP SPACE MISSIONS REVIEW

This chapter examines the second dataset of this research. In addition to ion and hall thruster best fit modelling, spacecraft design parameters influences the system-level optimization process. The inspected previous Moon and deep space missions are under 600 kg. Two exceptional cases are Dawn 1240 kg and NEAR Shoemaker 808 kg spacecrafts. In the dataset, Deep Space 1 and Dawn are two novel concepts have onboard ion engine through their journeys to the comets and asteroids. Smart-1 and Hayabusa had onboard hall thruster that were low cost Moon missions. Other spacecrafts in the dataset are Clementine, Grail, LADEE, Lunar Prospector and Stardust.

The critical approach is to gather both small satellite missions that flew to the Moon and small satellite missions which had onboard electric propulsion systems. Table 3.1, Table 3.2, and Table 3.3 presents inspected satellites with their, mass, volume, cost, tank mass, tank volume, payload mass and payload volume data. Best fit equations obtained from the Tables 3.1, 3.2 and 3.3 are listed in Appendix 2.

3.1 Data Analysis 1: Total Mass, Propellant Mass, Power and Cost

Best fit equations is found from Table 3.1 to represent the relationships between spacecraft system parameters. Both iterative and constrained optimization methods uses best fit equations comes from this relationship. In Table 3.1, the reference mission is Smart-1 which only consumed 82.5 kg xenon propellant with 366 kg initial spacecraft mass that cost $120M. The Smart-1 is the cheapest concept flew to the Moon by using hall thruster.

The Mars ODE mission is listed only for comparison between other missions. Mars ODE data is not considered in the optimization. Mars ODE mission is listed just in the Table 3.1 to compare other missions.

Table 3.1: Considered Moon and Deep Space Missions: Spacecraft Initial Mass, Spacecraft Total Power and Total Mission Cost Data

Satellite Name	$M_{propellant}(kg)$	$M_{total}(kg)$	$P_{total}(W)$	Total Cost ($M) in 2015
Clementine [24]	197	424	360	116.12
DAWN [25]	425	1240	1300	511.53
Deep Space 1 [7]	112.6	486.3	2500	221.07
Grail [26]	132.5	202.4	763	525.92
Hayabusa [8]	130	510	1200	96.83
Hayabusa -2 [27]	100	600	2600	133
Ladee [28]	134.8	383	295	284.38
Lunar Prospector [29]	138	296	202	91.45
MARS ODE [30]	350	727	1500	399.03
NEAR [31]	326	808	852	339.5
Smart-1 [9]	82.5	366.5	1850	120.3
Stardust [32]	85	385	330	283.46

3.2 Data Analysis 2: Spacecraft Volume to Tank Volume Ratio

Table 3.2 shows the relation between spacecraft volume and spacecraft propellant tank volume. There is one significant observation for electric propulsion missions that used xenon propellant. The volume ratios of Smart-1, Dawn, Hayabusa and Deep Space 1.

Table 3.2: Considered Moon and Deep Space Missions: Spacecraft Volume and Propellant Volume Data

Satellite Name	$V_{SC}(m^3)$	$V_{tank}(m^3)$	V_{SC}/V_{tank}
Clementine [24]	3.932	0.1641	23.951
DAWN [25]	3.6865	0.137	26.716
Deep Space 1 [7]	1.815	0.05695	31.870
Grail [26]	0.72	0.10147	7.0956
Hayabusa [8]	1.76	5.10E-02	34.5098
Hayabusa -2 [27]	4.12	0.228	18.070
Ladee [28]	8.11	0.13215	61.366
Lunar Prospector [29]	7.4376	0.1353	54.971
NEAR [31]	2.95	0.19	15.5263
Smart-1 [9]	0.68172	0.0266	25.6285
Stardust [32]	0.73	0.083	8.795

3.3 Data Analysis 3: Payload Mass, Payload Power, Solar Array Area

The payload mass, payload power and solar array area values of selected spacecrafts can be seen from the Table 3.3. The reference solar array area for the optimization is chosen as $10.3m^2$ which is the Smart-1 value. Spacecraft payload masses correspond around 5-6% of the total spacecraft masses. In addition, spacecraft payload powers correspond 1-20% of the spacecraft total powers. In the meantime, payload mass and power to total mass and power ratios are in good distribution that results precise best fit equations. The outstanding condition for electric propulsion missions is the total payload power is between 1.5-3% of the total power due to the high power demands of the ion or Hall thrusters. Therefore I use the same value as base during the optimization.

Table 3.3: Considered Moon and Deep Space Missions: Spacecraft Solar Array Area, Payload Mass and Payload Power Data

Satellite Name	$A_{solararray}(m^2)$	$P_{payload}(W)$	$M_{payload}(kg)$	Payload Power Percentage	Payload Mass Percentage
Clementine [24]	2.3	49.3	8.71	13.694	2.054
DAWN [25]	36.4	19	36.5	1.461	2.943
Deep Space 1 [7]	14.6	32.7	20.6	1.308	4.236
Grail [26]	3.76	75	40	0.98	1.976
Hayabusa [8]	12	57	15	4.75	2.94
Hayabusa-2 [27]	12	54.4	18.78	18.440	4.9033
Ladee [28]	4	17	23.7	8.415	8.0067
Lunar Prospector [29]	7.43	53	45	3.533	6.189
NEAR [31]	8.64	28	30	12.280	6.276
Smart-1 [9]	9.81	52.8	19	2.854	5.184
Stardust [32]	6.6	28	71	8.484	18.441

Chapter 4

LOW THRUST TRAJECTORY TRANSFER METHODOLOGY

4.1 The Earth - Moon System Geometry

The system-level optimization analyses two mission scenarios that are LEO departure and GEO departure. The initial inclination angle for LEO departure scenario is 28.5 degrees and the initial inclination angle for GEO departure case is 0 degree. Both mission cases have the final inclination of 76 degrees due to Earth-Moon system geometry for quasi-circular non-coplanar low thrust trajectory transfer. The Earth-Moon system geometry is illustrated in the Figure 4.1

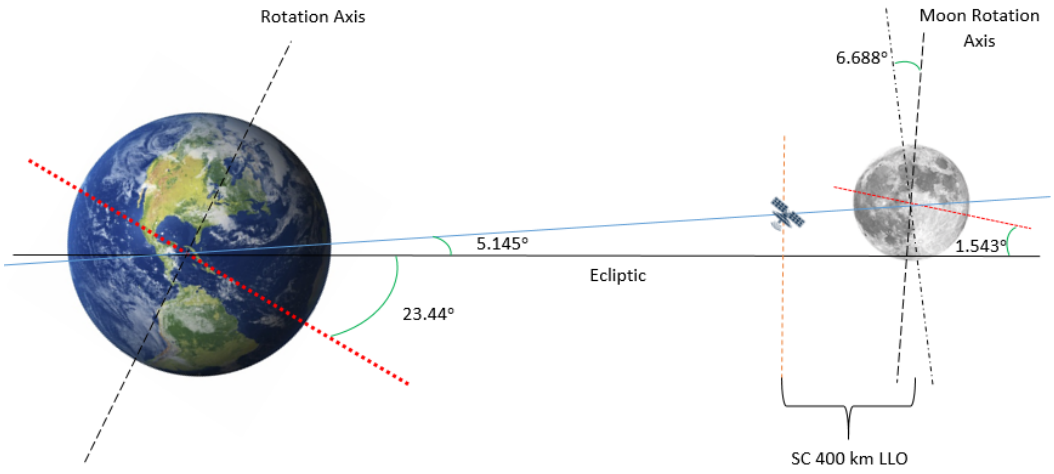

Figure 4.1: The Earth-Moon System Geometry

4.2 Low Thrust Trajectory Transfer Approaches

Electric thrusters provide very low thrust on the order of miliNewtons thus long flight time occurs. The orbit transfer by using electric propulsion systems must be spiraling trajectory transfer due to the low acceleration generation changing between 10^{-4} and 10^{-6}.

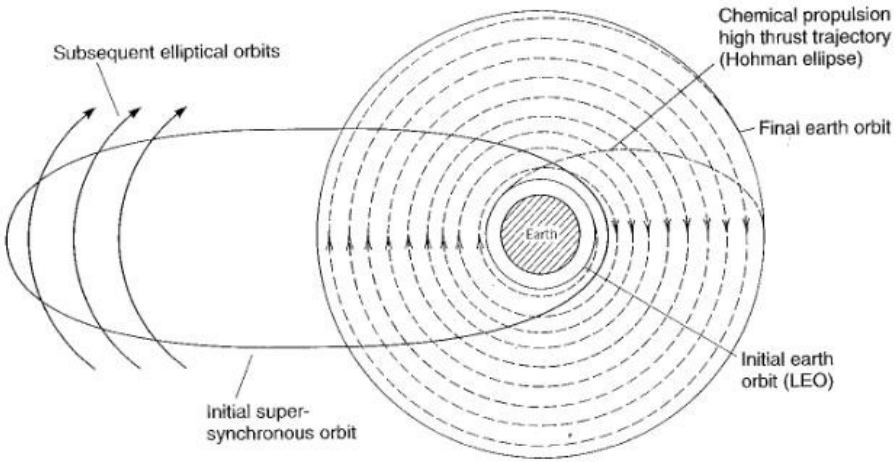

Figure 4.2: Spiraling Trajectory Transfers versus Hohmann Transfer Method [11]

The Figure 4.2 compares two types of spiraling low thrust trajectories with Hohmann transfer method. One type of low thrust trajectory illustrates circular orbit raising around the Earth as an initial case. The second type of low thrust trajectory case shows a highly elliptical and continuous orbit transfer. On the contrary Hohmann transfer method is provided by chemical propulsion system that high thrust moves the spacecraft from low Earth orbit to the higher orbit.

The mathematical analysis of spiral trajectory transfer requires various numerical optimization methods. To increase accuracy of the low thrust transfer trajectory, indirect or direct optimization methods by using Earth, Moon and Sun perturbations are significant approach. Instead of classical orbital elements, usage of equinoctial elements increase the precision of the results for ΔV and flight time. More advanced low thrust trajectory optimization studies can be found in [33, 34].

However, I consider the analytical method of Edelbaums low thrust transfer problem with optimal control theory [35] for the systems-level optimization. This analytical solution provides preliminary design case for small satellite Moon mission design and optimization [33].

4.3 Edelbaum's Low Thrust Transfer Problem with Optimal Control Theory

As stated in Chapter 4.2, the high specific impulse values of electric propulsion systems provide mili-Newtons of thrust due to the power limitations. Therefore, the low thrust transfer method which is derived by Edelbaum [35] is the remarkable approach for preliminary mission analysis to obtain high ΔV requirements. The analytic solution of low thrust transfer is valid for two quasi circular non-coplanar orbits. Assuming constant acceleration, constant propulsive thrust and constant thrust vector yaw angle, within each revolution, Edelbaum came up double valued inclination change and ΔV expressions [34]. Following, Kechichian [33] reformulated Edelbaums low transfer problem by using optimal control theory eliminated double-valued expressions for minimum transfer time between two non-coplanar orbits. Kechichian formed a single analytical expression that is valid for all transfer revolutions.

$$\tan \beta_0 = \frac{\sin\left(\frac{\pi}{2}\Delta i\right)}{\frac{V_0}{V_1} - \cos\left(\frac{\pi}{2}\Delta i\right)}, rad \tag{4.1}$$

First the initial out-of-plane yaw angle is calculated from the Equation (4.1). Subsequently, the Equation (4.6) calculates ΔV value requirement for the Earth-Moon transfers.

$$V_0 = \sqrt{\frac{\mu_{earth}}{R_0}}, {}^{m}/_{s} \tag{4.2}$$

$$V_f = \sqrt{\frac{\mu_{earth}}{R_f}}, {}^{m}/_{s} \tag{4.3}$$

Equations (4.2 and 4.3) are spacecraft initial and final velocities at the particular orbits.

$$R_0 = R_{earth} + h_0, km \tag{4.4}$$

$$R_f = R_{earth} + h_f, km \tag{4.5}$$

Spacecraft velocities can be found initial and final spacecraft altitudes by using Equations (4.4 and 4.5). For the inspected lunar mission, actual values of spacecraft altitudes and inclinations are presented in Table 6.1.

$$\Delta \mathrm{V} = \mathrm{V_0 cos}\beta_0 - \frac{\mathrm{V_0 cos}\beta_0}{\tan\left(\frac{\pi}{2}\Delta \mathrm{i} + \beta_0\right)}, {}^{km}/_{s} \tag{4.6}$$

The alternative way to calculate the ΔV budget is the Eq. (4.7) which is not dependent to the initial yaw angle.

$$\Delta \mathrm{V} = \sqrt{V_0^2 + V_1^2 - 2\mathrm{V_0 V_1 cos}\left(\frac{\pi}{2}\Delta i\right)}, {}^{km}/_{s} \tag{4.7}$$

In the iteration method, ΔV plays an important role for calculations of the flight time and the propellant mass. On the other hand, during the constrained optimization, ΔV does only influence the total flight time, ΔV has no role for minimization of spacecraft dimensions, spacecraft volume, total mass and propellant mass.

Chapter 5

SPACECRAFT SUBSYSTEM DESIGN METHODOLOGY

In this chapter I present the subsystem calculations used within the system-level optimization of the Moon mission. The optimum propellant tank pressure and mass values directly effects total initial mass calculation in the main optimization. In a similar manner the eclipse time is significant both for ΔV and the spacecraft battery mass calculations. Solar array design and battery selection determines critical parameters of system-level optimization such as spacecraft total power, solar array area and spacecraft volume.

5.1 Propellant Storage Tank Optimization

The propellant storage for the electric propulsion systems can be classified in two ways (i) cryogenic storage with a slow, but steady consumption and (ii) supercritical storage accompanied with light-weighted high pressure tanks. The cryogenic storages uses a room temperature gas for the feed allows propellant flow to cool the tank. The supercritical storage enhances the need of minimizing the tankage fraction by minimizing the propellant density [36]. In this thesis I estimated supercritical storage of the xenon gas for the system-level optimization to reduce the tank mass and volume size. Possible propellants for electric propulsion systems is presented in the Table 5.1.

The significant case for the electric propulsion supercritical storage is the ideal gas law presented in Equation (5.1) cannot be used at higher temperatures since the stored propellant is a noble gas. The classical tankage equation Equation (5.2) is not reliable for supercritical xenon storage. Therefore, an alternative approach is needed to overcome this situation.

Table 5.1: Electric Propulsion Propellant Types and Properties [36]

Parameter	**Argon**	**Krypton**	**Xenon**
$P_{critical}, kPa$	4864	5490	5838
$T_{critical}, K$	150.7	209.4	289.74
$\rho_{propellant}, kg/m^3$	1392	2412	3080

$$P = \rho RT/M \tag{5.1}$$

$$m_{tank} = m_{propellant}\frac{3P\beta\rho_{tank}}{2\sigma_{yield}\rho_{propellant}} \tag{5.2}$$

Various expressions have been embodied to find the minimum storage pressure and the density for corresponding tank mass and tankage fractions. One model is the Redlich-Kwong equations which gives consistent results with experimental data 32. Instead of the Equation (5.1), xenon propellant system uses the Equation (5.3).

$$P = \frac{RT\rho_{propellant}}{M - b\rho_{propellant}} - \frac{a\rho^2_{propellant}}{M(M + b\rho_{propellant})\sqrt{T}} \tag{5.3}$$

Redlich-Kwong parameters a and b are calculated from critical temperature and pressure values in Equation (5.4) and Equation (5.5).

$$a = \frac{R^2T^{5/2}_{critical}}{9(2^{1/3} - 1)P_{critical}} \tag{5.4}$$

$$b = \frac{(2^{1/3} - 1)RT_{critical}}{3P_{critical}} \tag{5.5}$$

Therefore, Equations (5.3, 5.4, and 5.5) are substituted into the Equation (5.2) to find the xenon propellant tank mass.

$$\frac{m_{tank}}{m_{propellant}} = \frac{3\beta\rho_{tank}}{2\sigma_{yield}}\left[\frac{RT}{(M - b\rho_{propellant})} - \frac{a\rho_{propellant}}{M(M + b\rho_{propellant})\sqrt{T}}\right] \tag{5.6}$$

Finally, from the derivation of the Equation (5.6) with respect to the propellant density $\left(\frac{\frac{\delta m_{tank}}{\delta m_{propellant}}}{\delta \rho_{propellant}} = 0\right)$, Equation (5.7) finds the minimum propellant density. Hence, the obtained density value used in the Equation (5.7) to find corresponding tank pressure within temperature values of 300K or 310K.

$$\rho_{propellant} = \frac{\sqrt{4RabM^2T^{3/2}} - RMbT^{3/2} - aM}{Rb^2T^{3/2} - ab} \tag{5.7}$$

5.2 Eclipse Duration Calculation

The eclipse fraction is calculated due to the spacecraft altitude at the apogee and the perigee. The Equation (5.8) results the twofold value of the actual eclipse fraction. Since the lunar mission is estimated as quasi-circular orbit, one half of the eclipse duration is considered in the Equation (5.12).

The maximum eclipse at both apogee and perigee can be calculated from fundamental cylindrical shadow analysis shown in the Figure 5.1.

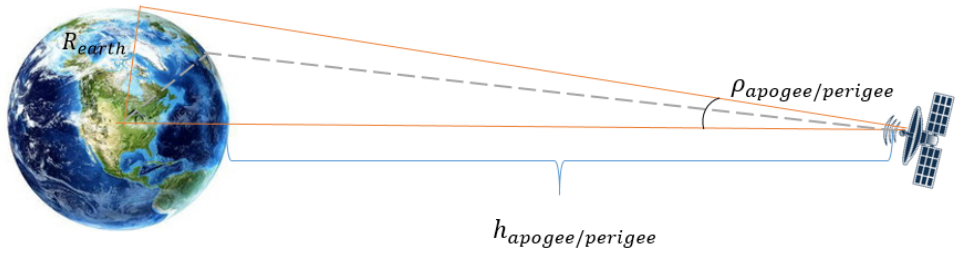

Figure 5.1: Angular Radius of Satellite with respect to the Earth [37]

$$E_{percentage} = \left(\frac{\rho_{apogee/perigee}}{180}\right) \times \left(\frac{R_{earth} + h_{apogee/perigee}}{a}\right) \tag{5.8}$$

$$\sin \rho_{apogee/perigee} = \frac{R_{earth}}{R_{earth} + h_{apogee/perigee}} \tag{5.9}$$

The Equation (5.8) demonstrates the eclipse fraction in percentage. Since I estimate near circular transfer orbits, the semi major axis, a is equals the spacecraft

altitude. Equation (5.9) defines the angular radius of the Earth, $\rho_{apogee/perigee}$ in degrees.

$$a = R_{earth} + \frac{h_{apogee} + h_{perigee}}{2} \tag{5.10}$$

$$P_{totalperiod} = 2\pi\sqrt{\frac{\left(R_{earth} + h_{apogee/perigee}\right)^3}{\mu_{earth}}} \tag{5.11}$$

During the Earth-Moon trajectory transfer, the total eclipse duration is found by multiplication of the Equations (5.10) and (5.11).

$$T_{eclipse} = E_{percentage} \times P_{totalperiod} \tag{5.12}$$

In the iterative optimization process, Equation (5.12) has significant role for the battery mass, total spacecraft mass and solar array power.

5.3 Solar Array and Battery Selection

Solar array design has shown progress since Vanguard I satellite that was the worlds first solar-powered spacecraft on March 1958 [38]. While early satellites were designed by using silicon solar cells that could only produce a few hundreds of power, modern solar arrays can produce kilowatts range of power with new designs. As Bailey and Rafaelle presented in their chapter [38] solar arrays are classified into six categories, (1) body-mounted arrays, (2) rigid panel planar arrays, (3) flexible roll-out arrays, (4) concentrator arrays, (5) high-temperature and intensity arrays and (6) electrostatically clean arrays.

In this study I consider the rigid and flexible roll-out arrays for the spacecraft design optimization. High specific power, low-cost and better area per power values of these arrays are the main elements for my consideration. The solar array characteristics of selected multi-juntion GaAs rigid and flexible designs are presented in the Table 5.2

For the battery design, I estimated rechargeable LiION batteries due to their highest energy densities. In addition, future energy density values of 250 to 400

Table 5.2: Space Solar Array Properties [37, 38]

Technology	BOL Specific Power (W/kg) @ Cell Efficiency	Cost per Watt ($/W$)	Cell Watts per square meter (W/m^2)	BOL Mass per square meter (kg/m^2)
TJ GaAs ultraflex	115 @26.8%	1-2K	383	2.8
TJ GaAs rigid	70 @26.8%	0.5-1.5K	383	2.8
CIGS Si Thin Film	275@ 11%	0.1-0.3K	191	2.3

(Whr/kg) are considered in the optimization process for the best scenario. Battery specifications are presented in the Table 5.3.

Table 5.3: Rechargeable Battery Characteristics [37]

Battery Performance Characteristics	**Ni-Cd**	**Ni-H2**	**LiIon**
Energy Density (Whr/kg)	30	60	125
Self-Discharge (% per day)	1	10	0.3

Eclipse time found from the Equation (5.12) and the battery mass in the Equation (5.6) are required to solar array parameters such as solar array mass and solar array area. Therefore, to end up solar array parameters Equations (5.13-5.15) are needed.

In the Equation (5.3), $T_{eclipse}$ is the eclipse period during the mission, $T_{daylight}$ is the daylight period of the mission. $T_{eclipse}$ and $T_{daylight}$values obtained from the Equations (5.8 and 5.9). In addition, $X_{eclipse}$ and $X_{daylight}$ are called path efficiencies between solar arrays and batteries. For the peak power tracking $X_{eclipse} = 0.60$ and $X_{daylight} = 0.80$ and for direct energy transfer $X_{eclipse} = 0.65$ and $X_{daylight} = 0.85$ [38]

$$P_{solararray} = \frac{\left[\frac{P_{eclipse}T_{eclipse}}{X_{eclipse}} - \frac{P_{daylight}T_{daylight}}{X_{daylight}}\right]}{T_{daylight}} \tag{5.13}$$

$P_{eclipse}$ is the spacecraft power during the eclipse period estimated as functional powers such as payload, communication, attitude determination and onboard computer. The $P_{daylight}$ is the spacecraft power during the daylight condition that is almost equal the spacecraft total power with solar array efficiency losses.

$$A_{solararray} = \frac{P_{solararray}}{P_0 I_d \cos(\theta)(1-D)^{t_{missiontime}}} \tag{5.14}$$

In the iterative optimization process solar array area is the key factor that mission time is held in the objective equation. The inherent degradation value 0.77. The solar incidence values 0 or 23.5 degrees due to the inclination changes. The initial power per unit area P_0 is the 383 $W/m^2$from the Table 8. For the GaAs the annual degradation D is the 5%. $t_{missiontime}$ is the total mission lifetime which can be considered equal to the SC flight time.

$$M_{solararray} = A_{solararray} \times 2.8 \tag{5.15}$$

The 2.8 kg/m^2 value taken from the in Table 5.2.

$$M_{battery} = \frac{P_{total} \times DOD \times T_{eclipse}}{(Whr/kg)_{battery}} \tag{5.16}$$

Another required parameter is the battery mass that depends on eclipse period, total spacecraft power, energy density and depth of discharge (DOD) value of the battery. The LiIon battery is estimated with the 125 (Whr/kg) energy density. DOD value could be from 40% through 60% [37].

5.4 The New SMAD Mass and Power Budget Assessment

The iterative optimization process in Figure 6.1 needs the relation between payload mass, subsystem mass, payload power and subsystem payload power. Therefore, the

relation between these parameters are estimated in the Table 5.4 taken from the New SMAD [37].

From the Table 5.4 it is observed that the payload mass is 23% of the subtotal mass, and payload power corresponds the 27% of the total SC power. These values are used in Figure 6.1 and directly influences main function of the iterative process.

Table 5.4: Spacecraft Mass and Power Budget Estimation [37]

Subsystem	**Mass Budget**	**Power Budget**
Payload	15	22
Structure & Mechanism	25	1
Thermal	6	15
Power	21	10
Attitude Determination	6	18
Command and Data Handling	4	11
Telecommunication	7	12
Propulsion	16	11

Chapter 6

SYSTEM-LEVEL OPTIMIZATION METHODOLOGY

6.1 Iterative Optimization Method

The iterative optimization process uses best fit equations obtained from Tables in Chapter 3 and Chapter 2. The objective funtion is formed by using ΔV value from Equation 4.7, propellant design parameters from Equation 5.6 and eclipse time from Equation 5.12. The Figure 6.1 shows the structure of the iterative optimization process accompanied with all inputs and free variables.

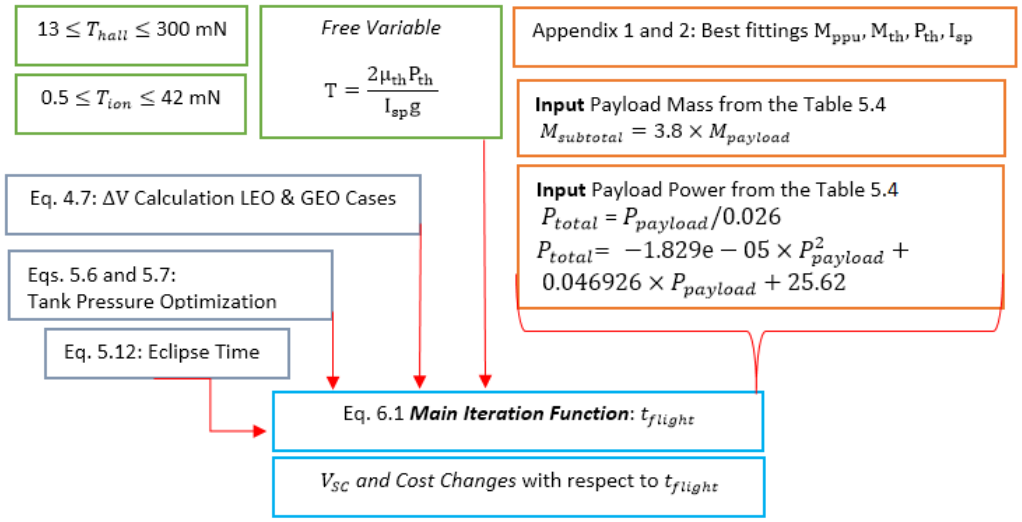

Figure 6.1: The iterative process lay-out

Spacecraft payload mass and power are selected as an input parameter. The $M_{subtotal}$ is the mass value excluding $M_{payload}$, $M_{propellant}$, $M_{solararray}$, $M_{battery}$ and the M_{tank}, M_{th} (thruster mass) and the M_{ppu} (thruster PPU mass) masses. The main reason of subtotal mass definition is to distinguish other subsystem masses

from the calculated masses. Other subsystem masses such as command and data handling, attitude determination and control, thermal management, communication and structure are estimated from the Table 5.4.

The objective function of the iterative process which is the flight time depends upon the propellant mass and the propellant mass flow rate in the Equation (6.1).

$$t_{flight} = \frac{M_{propellant}}{\dot{M}_{propellant}} \tag{6.1}$$

The propellant mass flow rate is calculated from the Equation (6.2). T is the thrust level of the ion or hall engine that is free variable. Specific impulse I_{sp} is calculated from best fitting equations in Appendix 1 and Appendix 2.

$$\dot{M}_{propellant} = \frac{T}{I_{sp}g} \tag{6.2}$$

ΔV budget comes from the fundamental rocket equation in Equation (6.3). The Equations (6.2 and 6.3) are substitute into the Equation (6.1) to form the objective function.

$$\Delta V = I_{sp}gln\left[\frac{M_{propellant} + M_{dry}}{M_{propellant}}\right] \tag{6.3}$$

The objective function in Equation (6.4) depends upon solar array mass, xenon propellant tank mass, battery mass and ΔV budget.

$$t_{flight} = \frac{\left(e^{\Delta V/I_{sp}g} - 1\right) \times [M_{solararray} + M_{battery} + M_{subtotal} + M_{tank}]}{T/I_{sp}g} \tag{6.4}$$

The solar array mass is defined in Equation (6.5) and is substituted into the Equation (6.4) for the final form of the objective function. The margin for the flight time, t_{marg} could be estimated from 5 to 10 days due to the mission design.

$$M_{solararray} = \frac{P_{solararray} \times 2.8}{P_0 I_d \cos(\theta)(1-D)^{t_{flight}+t_{marg}}} \tag{6.5}$$

Therefore the final form of the iterative objective function is presented in the Equation (6.6).

$$t_{flight} = \frac{\left(e^{\Delta V/I_{sp}g} - 1\right) \times \left[\frac{P_{solararray} \times 2.8}{P_0 I_d \cos(\theta)(1-D)^{t_{flight}+t_{m\,\mathrm{arg}}}} + M_{battery} + M_{subtotal} + M_{tank}\right]}{T/I_{sp}g} \tag{6.6}$$

6.2 Constrained Optimization Method

The constrained optimization process uses the fundamental fmincon tool of the MATLAB. The objective of the optimization is to find optimum spacecraft volume for a reliable lunar mission with maximum payload mass. The hexagonal spacecraft structure is estimated that enables more volume compared to cubic structure.

The initial values, lower and upper bounds of spacecraft dimensions and propellant tank are listed in Table 6.1. The parameter h is the hexagonal spacecraft height, a is the side length of the spacecraft and the r_{tank} is the radius of the propellant tank.

Table 6.1: The constrained optimization process initial values

Unit is *meters*	$x_1 = a$	$x_2 = h$	$x_3 = r_{tank}$
Initial values	0.7	0.8	0.3
Lower bounds	0.3	0.5	0.1
Upper bounds	1	1.2	0.6

The constraints of the optimization are listed in Equation group 6.7. The spacecraft volume to propellant tank volume ratio of selected electric propulsion mission is taken from the Table 3.3. The upper bound of the spacecraft power is 1600W, total spacecraft mass 400kg and the propellant mass 120kg.

$$25 \leq \frac{V_{SC}}{V_{tank}} \leq 35, P_{total} \leq 1600, M_{total} \leq 400, M_{propellant} \leq 120 \tag{6.7}$$

The objective function of this process is found from the Equation 6.8. The flight time depends on the dry mass of the spacecraft and ΔV of the selected mission case.

$$t_{flight} = \left(\frac{I_{sp} \times g \times 1000}{T} \right) \times M_{dry} \times (e^{\frac{\Delta V}{I_{sp} \times g}} - 1) \tag{6.8}$$

The dry mass of the spacecraft is the explained in Equation 6.9 that is the sum of subtotal mass and other calculated subsystem masses.

$$M_{solararray} + M_{tank} + M_{battery} + \ M_{subtotal} \ = \ M_{dry} \tag{6.9}$$

Main equations are listed in Equations (6.10-6.12). Optimized values of the spacecraft volume, solar array area and propellant tank volume are required to find the objective function.

$$V_{SC} = 1.5\sqrt{3}x_2{x_1}^2 \tag{6.10}$$

$$A_{SA} = 6x_1x_2 + 3\sqrt{3}{x_1}^2 \tag{6.11}$$

$$V_{tank} = (4/3)\pi{x_3}^3 \tag{6.12}$$

Equations (10.1, 10.2 and 10.3) in Appendix 3 are best fitting equations obtained from the Tables 3.1, 3.2 and 3.3. These equations are substituted into the constraints and the objective function for the optimization.

Chapter 7

SYSTEM-LEVEL OPTIMIZATION RESULTS

7.1 Constant Mission Parameters

Constant mission parameters in the Table 7.1 explains initial and final altitudes of the spacecraft around the Earth and the Moon during the trajectory transfer. While the initial altitude is chosen as 700 km for the LEO departure case, the initial spacecraft altitude is estimated as 35000 km for the GEO departure case. For the both cases, the final spacecraft altitude is 400 km low lunar orbit (LLO) with the moon inclination of 76 degrees. In addition, initial inclination values are taken as 28.595 degrees for LEO departure case and 0.005 degrees for the GEO departure case.

Furthermore, a spherical titanium propellant tank is estimated with the yield strength of 1.4e9 Pa. The β is the safety factor could be 2 for titanium tank.

Table 7.1: Constant and Input Mission Parameters

R_{earth}, km	R_{moon}, km	$\mu_{earth}, \mu_{moon}, {km^3}/{s^2}$	h_{LLO}, km
6378.14	1737.4	398600.44, 4902.799	400
i_{LEO},i_{GEO}, deg	i_{moon}, deg	h_{LEO}, km	h_{GEO}, km
28.595, 0.005	76	700	35000
σ_{yield}, Pa	$\rho_{titanium}, kg/m^3$	β, constant	$R_{gasconstant}$, J/(kgmolK)
1.4e9	4850	2	8.314

7.2 Propellant Tank Optimization

The propellant is xenon gas which can be stored at 300K or 310K. I consider 300K xenon storage temperature that results lower pressure and thus lighter propellant tank mass. Due to Equations (5.3-5.7) propellant tank optimization results are presented in the Table 7.2. Also the Figure 7.1 shows the optimum propellant tank density value with respect to minimum tankage fraction at 0.0638.

Table 7.2: Propellant Tank Optimization Results for 300K and 310K

T, K	$\rho_{propellant}, kg/m^3$	P, MPa	Tankage Fraction $(m_{tank}/m_{propellant})$
300	1350	8.3	0.0638
310	1310	9.8	0.0782

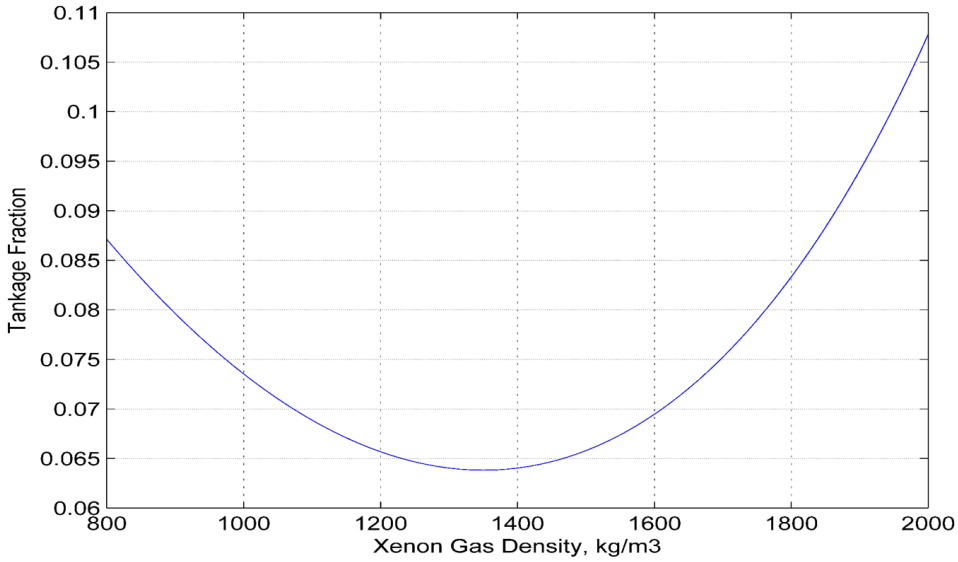

Figure 7.1: Tankage Fraction versus Xenon Tank Density

7.3 Eclipse Duration of the Moon Mission

The Figure 7.2 shows as the spacecraft altitude increases the eclipse time increases up to the 12000 seconds, 3.33 hours. This is the twofold value of the actual eclipse time as explained in Chapter 5.2. Therefore the overall eclipse duration is 1.5 hours.

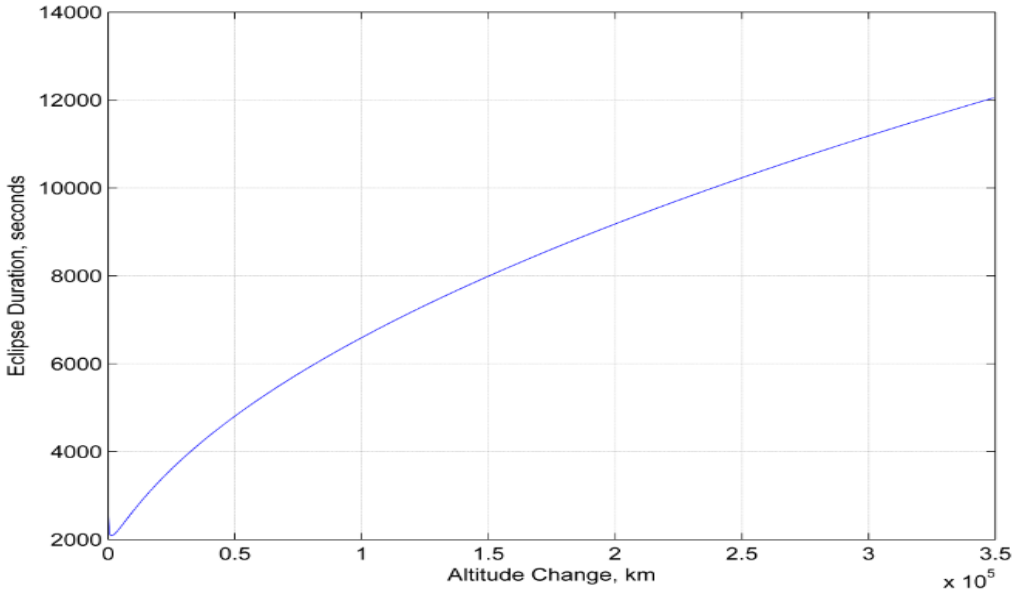

Figure 7.2: Eclipse Time versus Spacecraft Altitude Change

7.4 Iterative Optimization Results

7.4.1 ION Thruster GEO Departure Case

The Table 7.3 shows all parameters of GEO departure mission case by using ion thrusters. Due to the mission parameters optimized flight time is 1200 days with 205 kg total spacecraft mass. Although I obtain 26 kg less propellant than the value used for the Smart-1 mission, the flight time is quite long with 1200 days. The total mission cost is \$108M which is \$4M cheaper than the Smart-1.

The Figure 7.3 shows the initial mass change of the spacecraft due to the engine thrust values. The total mass change is only 2 kg. Therefore the deficiency of this

Table 7.3: GEO departure mission case results by using ION thruster

T, mN	M_{total}, kg	$M_{propellant}, kg$	V_{SC}, m^3	V_{tank}, m^3	V_{SC}/V_{tank}
16	**205.39**	**56.43**	**0.6705**	0.0179	37.46
P_{SC}, W	M_{dry}, kg	A_{SA}, m^2	M_{SA}, kg	Total SC Cost, $M	$t_{flight}, days$
800	148.96	**8.755**	8.79	**108.365**	**1200**

iterative optimization process is that mission parameters acts as system outcomes, there are not optimized anymore.

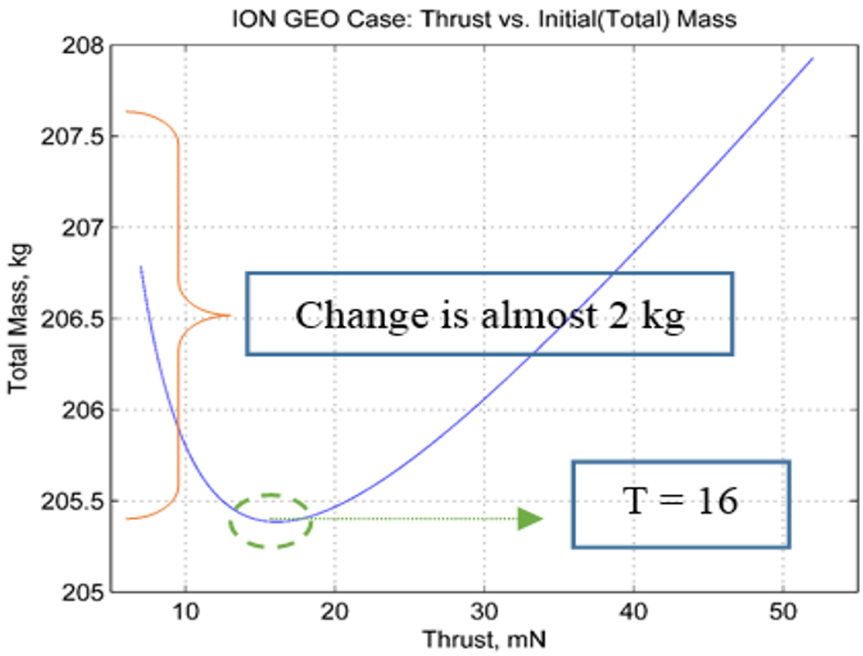

Figure 7.3: Spacecraft Initial Mass Change versus ION Engine Thrust Value

7.4.2 ION Thruster LEO Departure Case

For the ion engine LEO case in the Table 7.4, volume ratio is 35 which is remarkable. This mission case is the cheapest mission compared with the all considered missions in the Table 3.1. the xenon propellant consumption is 64 kg that is 20 kg less than

the SMART-1 mission. Spacecraft volume is reasonable with $0.7m^2$.

Table 7.4: LEO departure mission case results by using ION thruster

T, mN	M_{total}, kg	$M_{propellant}, kg$	V_{SC}, m^3	V_{tank}, m^3	V_{SC}/V_{tank}
23	**213.97**	**63.95**	**0.7078**	0.0201	35.2139
P_{SC}, W	M_{dry}, kg	A_{SA}, m^2	M_{SA}, kg	Total SC Cost, $M	$t_{flight}, days$
800	150.02	8.49	8.859	**110.964**	**980**

The same iterative optimization deficiency can be shown in Figure 7.4. Total mission cost change is not considerable due to the spacecraft volume change.

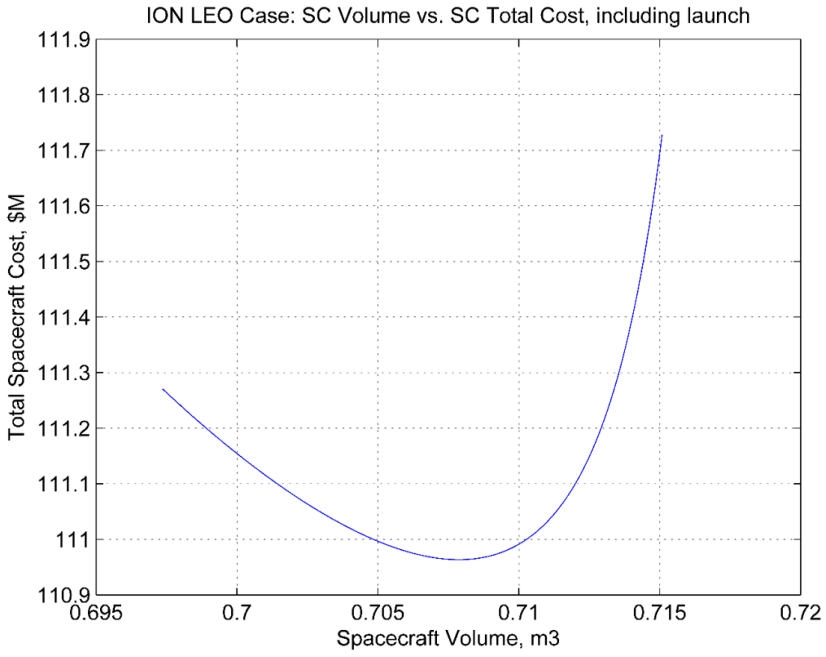

Figure 7.4: Spacecraft Total Cost Change versus Spacecraft Volume Change

The main reason to show only volume and cost relation is other parameter relations have the same deficiency therefore only one relation is enough to understand the iterative optimization process deficiencies.

7.4.3 HALL Thruster GEO Departure Case

From the Table 7.5, total mission duration is 165 days that is significant result for low thrust missions. However the solar array area is $12.75m^2$ which is a design issue. The required propellant mass is 65 kg that is almost same value with the LEO departure ion thruster case. Ion engine case is slower but cheaper than hall engine case.

Table 7.5: GEO departure mission case results by using HALL thruster

T, mN	M_{total}, kg	$M_{propellant}, kg$	V_{SC}, m^3	V_{tank}, m^3	V_{SC}/V_{tank}
77	**229.52**	**65.26**	**0.7145**	0.0188	38
P_{SC}, W	M_{dry}, kg	A_{SA}, m^2	M_{SA}, kg	Total SC Cost, $M	$t_{flight}, days$
1351	164.26	**12.75**	14.13	**115.7**	**165**

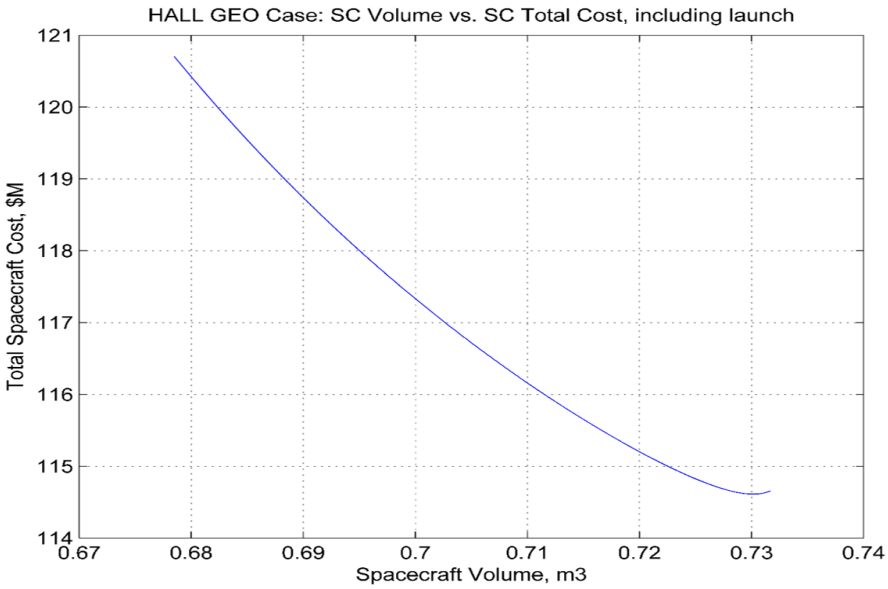

Figure 7.5: Spacecraft Total Cost Change versus Spacecraft Volume Change

The Figure 7.5 has the similar deficient character in comparison with Figure 7.4 and Figure 7.3. The spacecraft volume change is not considerable with respect to the total spacecraft cost.

7.4.4 HALL Thruster LEO Departure Case

The Table 7.6 presents the mission parameters that have 45 days and $5M increase compared with GEO departure case. In addition the xenon propellant consumption requirement is 82 kg. Therefore, this mission case is not feasible. In addition the Figure 7.6 has the same undesirable distribution that the spacecraft volume is just an outcome.

Table 7.6: LEO departure mission case results by using HALL thruster

T, mN	M_{total}, kg	$M_{propellant}, kg$	V_{SC}, m^3	V_{tank}, m^3	V_{SC}/V_{tank}
77.3	**247.76**	**82**	**0.8003**	0.0213	37.57
P_{SC}, W	M_{dry}, kg	A_{SA}, m^2	M_{SA}, kg	Total SC Cost, $M	$t_{flight}, days$
1351.5	165.76	**12.86**	14.15	**121.3**	**208.2**

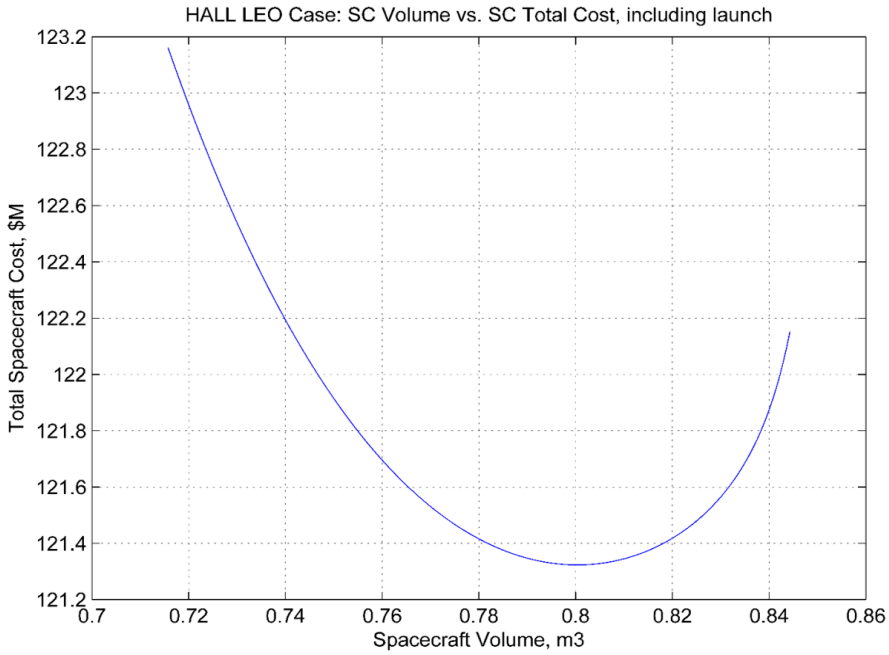

Figure 7.6: Spacecraft Total Cost Change versus Spacecraft Volume Change

7.5 Constrained Optimization Results

Although the iterative optimization method gives consistent results for system-level mission parameters, outcomes are not optimized. To overcome inconsistent outcomes of the optimization an alternative method is needed to understand mission profile in proper way.

The objective of the constrained optimization is to find optimum spacecraft volume value for the lunar mission. The optimized spacecraft volume is $1.47m^3$ with a hexagonal spacecraft architecture design. This allows up to 121.6 kg payload mass. Due to the mission design, payloads could be an external CubeSats or mini-rovers. The total spacecraft mass is found around 400 kg that increases the total cost through $170M.

Unlike the iterative method, this optimization process presents the same results both LEO and GEO departure mission cases. Both cases consumes same amount of propellant through the Moon that the total flight duration only changes. Differences of the flight times for the hall thruster case are presented in Figure 7.7 and Figure 7.8.The ion engine case demonstrates excessive mission durations over 1000 days, only the hall engine type is presented.

Table 7.7: Hexagonal Spacecraft Volume Constrained Optimization

$h, meters$	$a, meters$	$r_{tank}, meters$	$M_{propellant}, kg$	P_{SC}, W	$M_{payload}, kg$
0.9372	**0.7764**	**0.2896**	**119.4411**	885.8672	up to 121.6
V_{SC}, m^3	A_{SA}, m^2	V_{tank}, m^3	M_{tank}, kg	M_{total}, kg	Total SC Cost, $M
1.4678	**7.50**	0.107	6.33	**397.38**	**169.815**

In conclusion, in order to determine how much payload mass is required to accomplish the intended objections, payload size and the mission cost could be tradeoffs.

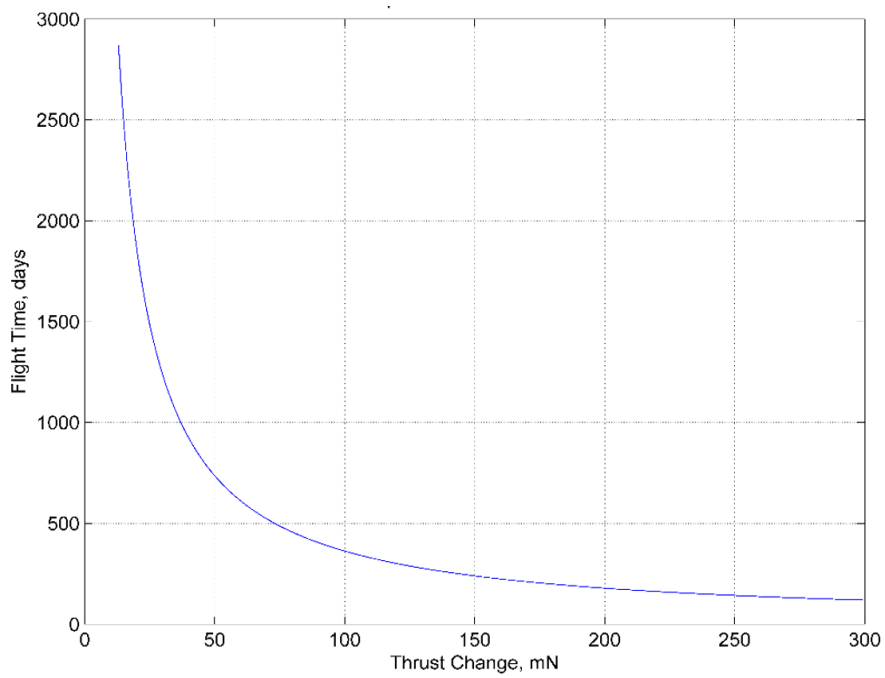

Figure 7.7: Spacecraft Volume Optimization LEO Case Flight Time versus HALL Thrust

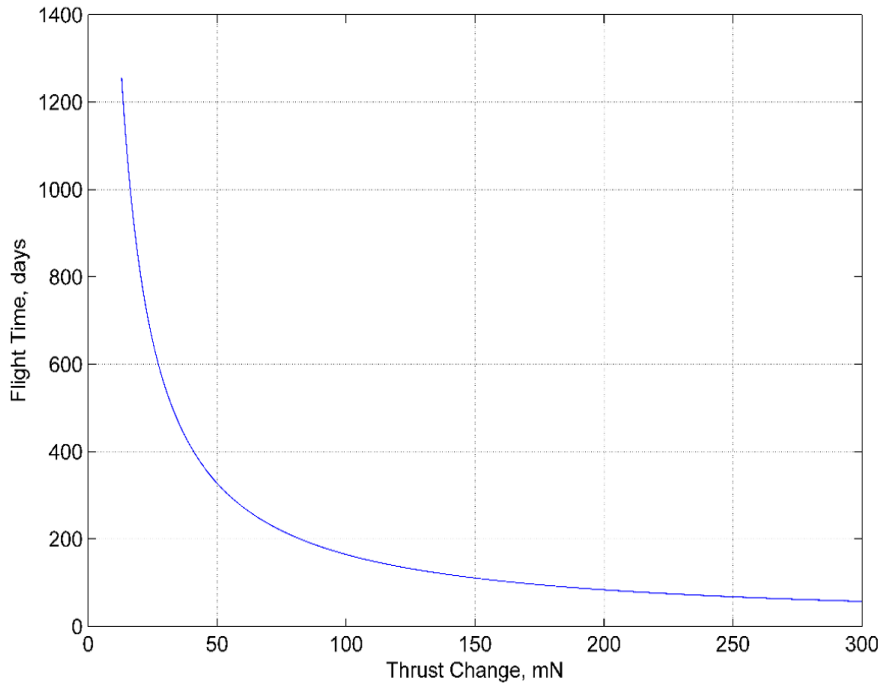

Figure 7.8: Spacecraft Volume Optimization GEO Case Flight Time versus HALL Thrust

Chapter 8

MISSION COST ASSESSMENT: SPACE ECONOMY OF TURKEY

8.1 Turkish Space Sector Review

Turkey has ability of developing, producing and operating communication satellites, Earth observation satellites and scientific CubeSats. BILSAT and RASAT are two important Earth observation satellites of the Turkey. BILSAT is the first Earth observation satellite that is produced by corporation between Turkish Space Technologies Research Institute (TUBITAK-UZAY) and Survey Satellite Technology Limited. BILSAT was launched in 27 September 2003. Turkish earth-observation satellite named Gokturk-2 was launched from Jiuquan, China in 2012. The satellite designed and built by TUBITAK's space technologies research unit, TUBITAK-UZAY, in cooperation with Turkish Aerospace Industries (TAI). Gokturk-2 is Turkey's second national earth observation satellite. RASAT is another satellite that has electro-optic camera which also was developed by TUBITAK-UZAY and launched from Russia on Aug. 17, 2011 [39].

TURKSAT has lead the communication satellite launches from 1994 with Türksat-1B. Latest communication satellite Türksat-4B was launched in February 2014 which the satellite produced by MELCO. Moreover, TURKSAT is planning to develop Türksat-5A communication satellite with using national sources [40].

Göktürk-1 project is coordinated by Turkish under secretariat for defense industries. Prime contractor is Telespazio and Thales Alenia Space. Göktürk-1 has electro-optic camera with under-meter resolution. Personnel of the Turkish Aerospace Industry (TAI) joined all engineering activities to gain experiences. In addition, Göktürk-2

was launched in 2012 from China. It has 2.5 meters military observation camera and developed by the corporation of TAI and TUBITAK-UZAY. The latest military observation satellite project is Göktürk-3 which is planning to launch in 2019. Main contractor of the project is TAI and project is coordinating by Turkish undersecretariat for defense industries. Sub-contractors are ASELSAN and TUBITAK-UZAY [40].

ITUpSAT-1 and TURKSAT-3USAT were two main nanosatellite that performed by university students. ITUpSAT-1 is produced by Istanbul Technical University (ITU) and launched in September 2009. ITUpSAT-1 is the first pico-satellite that developed by a university in Turkey. TURKSAT-3USAT is launched in 2013. It's a LEO communication triple unit CubeSat that produced by TURKSAT and ITU [41].

BeEagleSat satellite is the current CubeSat project from Istanbul Technical University as a part of the QB50 project that will planning to launch in 2016 [42].

Turkey's procurement agency Undersecretariat for Defense Industries (SSM) signed a contract with the country's national missile manufacturer, ROKETSAN, to build the Turkish Satellite Launching System (UFS) for pre-conceptual design phase on July 17, 2013 [43]. Turkey made successful launches from other launch sites. Furthermore, in order to gain the satellite launch capability to reach the space independently with the aim of supporting the sustainability of Turkish satellite programs, the project was entered into force. By the help of this project, satellite launch vehicle development, establishment of satellite launch center, remote earth stations and related service procurements will be achieved.

By the help of the UFS, Turkey will be capable of launching, initially, satellites into low earth orbit (LEO) through a launching center the company will build and the Turkish Air Force will operate. Turkey will then become one of the countries capable to produce, test and launch its own satellites.

Prominent companies that improve the Turkish space industry especially in the satellite production field are TAI, TUBITAK Space, ROKETSAN, TURKSAT, ASELSAN and HAVELSAN. Also there are many small-medium size enterprizes (SME) in

the field of aerospace in Turkey. As an example of this SMEs, GUMUSH Aerospace and Defense Ltd. is the first pico and nano satellite design and manufacturing company for academic and civil industrial use in Turkey and Middle East Region [44].

Istanbul Technical University (ITU), Middle East Technical University (METU), University of Turkish Aeronautical Association (UTAA), Ondokuz Mayis University and Gaziantep University have aeronautics and astronautics department. In addition, some universities will going to form new Aerospace departments in near future. Undergraduate students are well educated after a qualified four year university education.

Undergraduate student projects like CanSat, model rocket and aircraft activities are bring those experiences in PDR, CDR, team work, self-confidence, cost planning, project management and organization. The most significant reason why students move away from space sector is the cultural aspects and lack of space inspiration.

8.2 Global Space Economy Survey: OECD Space Economy 2014 Report

The country based investigations of the space sector is helpful to form international collaborations. In addition, understanding global value chains, R&D budgets, human capital, spin-offs and outputs in the economy are significant to create more corporate structure in organizations and agencies. The global space sector employed more than 900,000 persons around the world in 2013, including space agencies, defense-related organizations, the space manufacturing industry and commercial telecommunication companies, excluding universities and research institutions [45]. As can be seen from the Figure 8.1, the objective of space industry is to increase investments and business in global scale. Figure 8.1 is the global space revenue distribution in 2013 that was $256.3 Billion.

Space related investments, academic publications and R&D studies are increasing in Turkey. Figure 8.2 shows the patent application amount for space related technologies per country. Although Turkey has an incremental share of applicants betwee 2009 and 2011, the global level of Turkey is not as it should be.

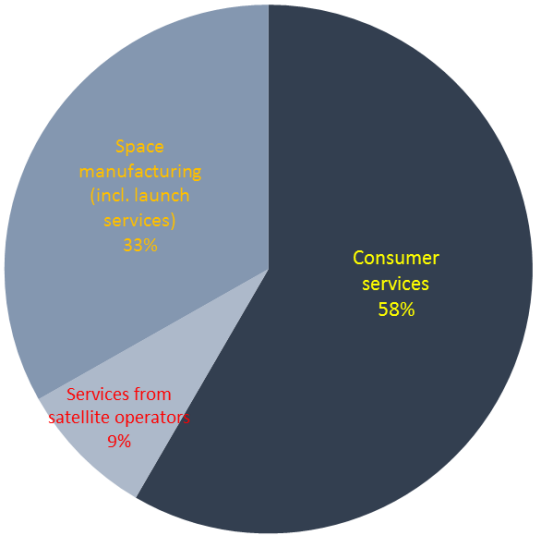

Figure 8.1: Main Drivers of the Space Economy [7]

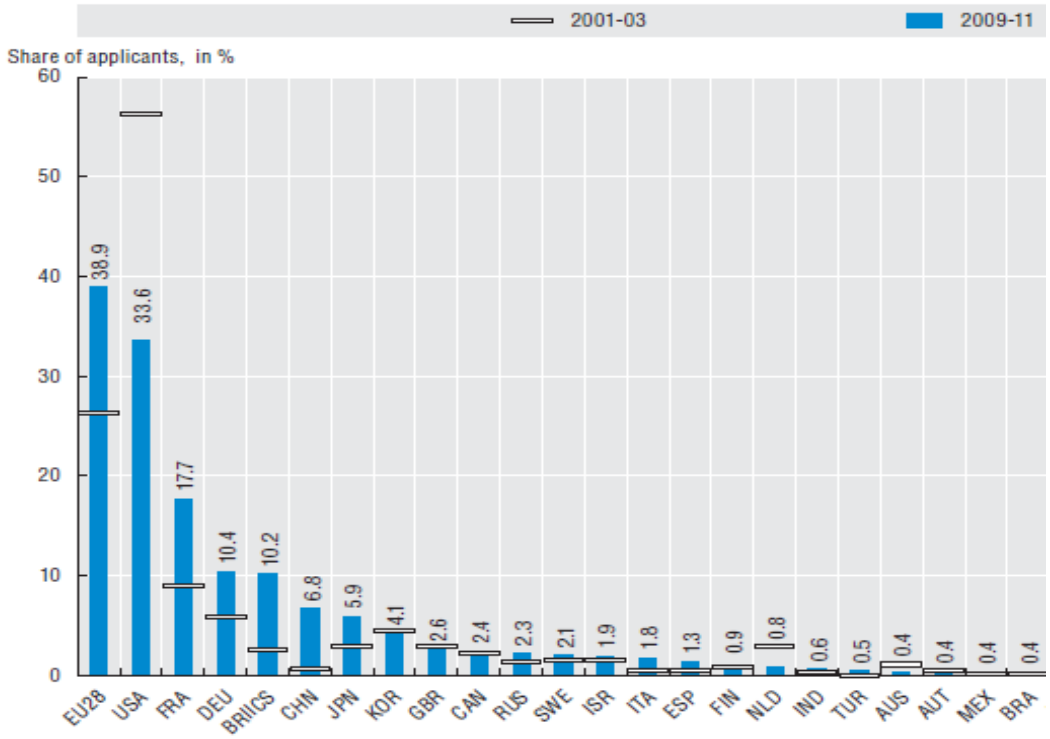

Figure 8.2: Patent Applications for Space-Related Technologies per Economy [45]

Furthermore the Table 8.3 presents the scientific production in satellite technologies per country in 2003 and 2013. Turkey has 1.3% share of publications level that is gradually increasing with the new small satellite researches.

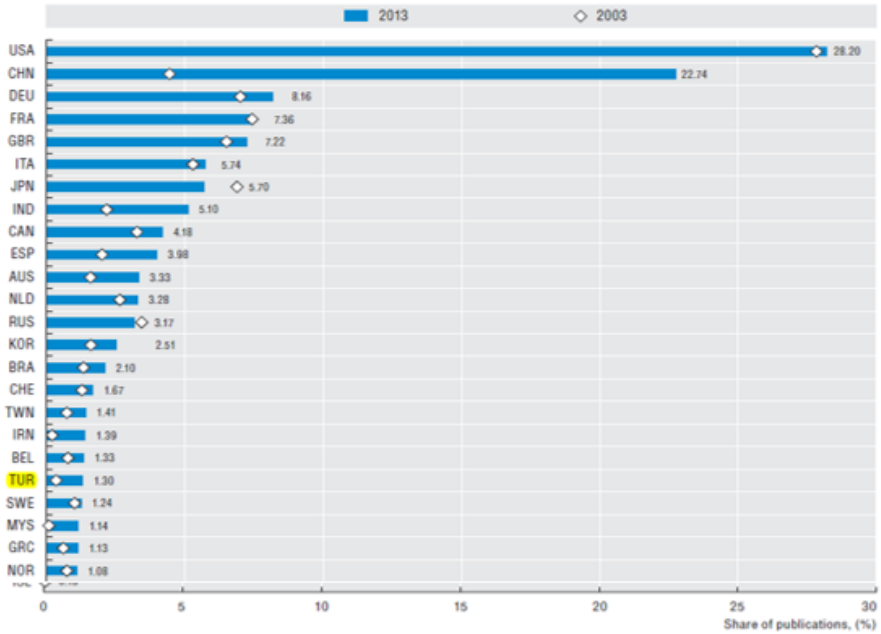

Figure 8.3: Scientific Production In Satellite Technologies per Country [45]

8.3 Turkish Space Economy Review: Small Satellite Investment

Space missions in the past were mainly focused on large satellites, but are now transitioning to smaller satellites. This trend is the result of the cost reduction and advances in technology, which allows the miniaturization [46]. Small satellites put a limit for developing and manufacturing due to dimension limitations; however, there are many benefits of small satellites. The possibility of testing subsystems in space can be given as one of the most important benefits.

Turkey plans to send into orbit a total of 16 satellites by 2020, according to the government roadmap for military and civilian satellites [47]. The subsystems of satellites are mostly ready to use, however, in order to gain a high fidelity and

sustainability for manufacturing, there is an emerging to prove these systems in orbit. Also, an interplanetary or moon mission by using small satellites shall expedite the process of space technology development.

Turkey has allocated approximately $200 million budget for R&D and infrastructure development in the last 5 years[10]. Aerospace (aviation and space) sector covers only 3% of total R&D budget. Automotive industry has 30% of R&D and defense industry holds around 8%. According to the 2023 Turkey Export Strategy and Action Plan, 2% of total $2 trillion of GNP will be allocated for R&D budget [48]. At least 2% of total R&D budget means approximately $400 million. The possible approximation of the demanding investment budget for space technology is shown in Fig. 8.4.

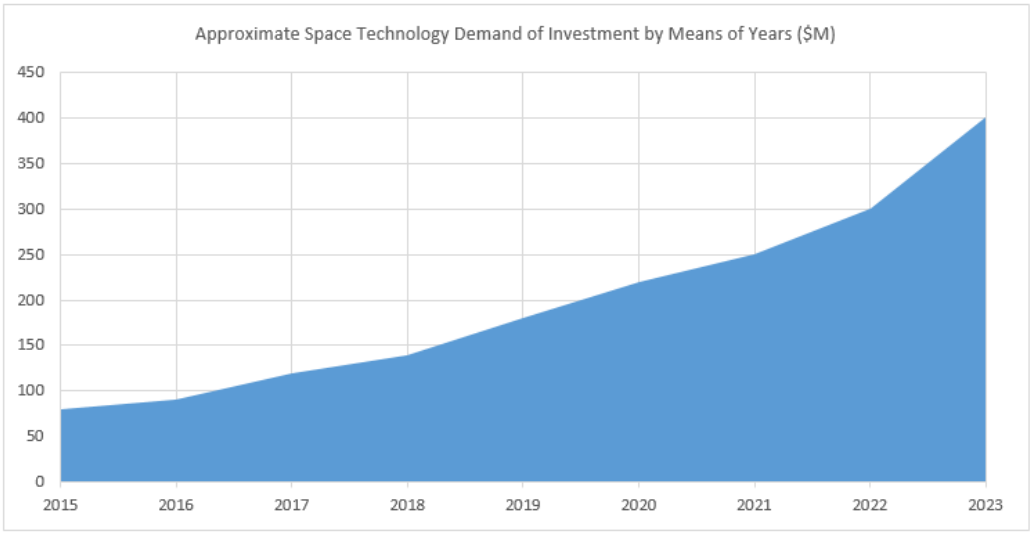

Figure 8.4: Approximate space technology demand of investment by means of years [48]

8.4 Cost Assessment: System-Level Lunar Mission Case Result

Case study is the iterative optimization of a hexagonal spacecraft architecture. The iterative method with LEO departure ion thruster has 23 mN with minimum 213 kg total mass. Corresponding spacecraft volume is 0.70 m^3, propellant mass is 64 kg.

This scenario cost $108.5M and takes 980 days. Same thruster level for GEO departure case takes 880 days with 58 kg xenon gas. The total cost reduces $2.5M. For HALL engine design, LEO departure case needs 0.8 m^3, 247 kg spacecraft including 82 kg xenon. 77 mN thrust operates 208 days towards the Moon that ends up with $121M total cost. If the spacecraft to be launched from GEO, flight time reduces 45 days by consuming 65 kg propellant. For GEO launched HALL case, total spacecraft mass and volume values are 230 kg and 0.71 m^3 which cost $115M.

Table 8.1: The Summary of Lunar Mission Cases from the System-Level Optimization

Parameter	IONLEO Case	ION GEO Case	HALLLEO Case	**HALLGEO Case**
Optimum Thrust, mN	23	23	77	**77**
Flight Time, days	980	880	208	**163**
Propellant Mass, kg	64	58	82	**65**
Total SC Volume, m^3	0.70	0.67	0.8	**0.71**
Total SC Mass, kg	213	210	247	**230**
Total Cost, $M	108.5	106	121	**115**

According to the Table 8.1, spacecraft by using ion propulsion and departures from GEO produces the lowest cost. For the same spacecraft if we use the HALL thrusters total mission cost increases around $5M and flight time reduces around 700 days. That is the significant trade-off for the mission design.

Chapter 9

CONCLUSION AND DISCUSSION

The HALL thruster case has better outcomes in comparison with the ion engine case. Hall thruster operates higher power levels which means smaller mission duration and larger solar arrays. Mission cost and mission duration can be considered as mission trade-offs. Hall engine cases in Table 7.5 and Table 7.6 show that the total mission cost including development, launch and operational costs increase around $9M in comparison with ion engine cases. In contrast to cost, flight time reduces almost factor of 10 in GEO departure scenario and factor of 6 in the LEO departure type. Therefore although mission cost increases a potential lunar mission could be designed by using hall thrusters especially higher than 70mN thrust value due to short mission time.

The iterative optimization process gives an overall understanding of lunar mission parameters, but still it has undesirable outcomes. Change in mission parameters is not considerable can be shown in Figures 7.3, 7.4 and 7.5. The alternative method, constrained optimization process overcomes inaccurate results with a different approach. This method finds the optimum spacecraft volume for the hexagonal structure. Due to the results in Table 7.7, the optimized spacecraft allows up to 121 kg payload mass which is significant advantage for a lunar mission. The mission designer is free to manage the payload for various kinds of lunar mission objectives. However in this time the mission cost increases more than $50M compared to iterative optimization results.

Following steps to ameliorate the system-level optimization for a small satellite deep space mission would be involvement of advance subsystem analyses. First, low thrust trajectory transfer analysis in this research is quite fundamental. The essential

improvement should be the direct or indirect optimization including moon resonances for elliptical low thrust orbits. Therefore the improved Earth shadow analysis with entry and exit positions are needed. Cryogenic storage of xenon propellant would be another improvement for an advanced spacecraft design. Cost analysis by using NASA Cost Estimating Handbook is significant in order to bring down the mission cost from $100 millions through $50 millions.

Another goal of that study is to discuss the lunar mission cost obtained by the system-level optimization research for the Turkish space economy. There is incremental trend in space technology demand investment by means of years. The total R&D budget will be around $400M. Therefore a small satellite Moon mission with a possible cost of $100M seems a challenging goal. Turkey needs more small and medium size enterprises within the space sector. The main deficiency of the space sector is the collaboration of universities, government and the private sector. The government should support the private sector and should provide more funding. In the meantime companies should be in collaboration with universities. There is a clear gap between universities and the companies.

In addition, the academic profile of Turkey is presented from the OECD report in Figures 8.2 and 8.3. Although patent applications for space-related technologies and scientific productions in satellite technologies are rising within the last five years, the level is not as it should be in order to generate high level missions such as rover missions, space robotics, lunar and Mars orbiters.

The next step for Turkey should be creation of significant fields (1) project based university education, (2) national/international long-term internship opportunities, (3) relations between students and young professionals, (4) leadership and knowledge management programs within companies and (5) public outreach activities to foster space in the society.

Chapter 10

APPENDIX

10.1 Appendix 1: ION Thruster Best Fitting from Table 2.2

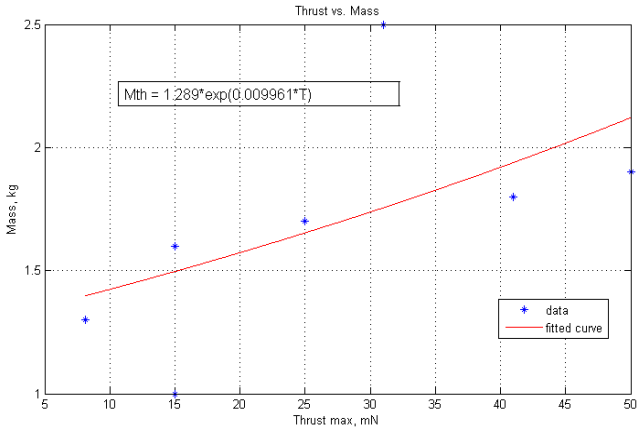

Figure 10.1: Thrust versus Thruster Mass Best Fit from the Table 2.2

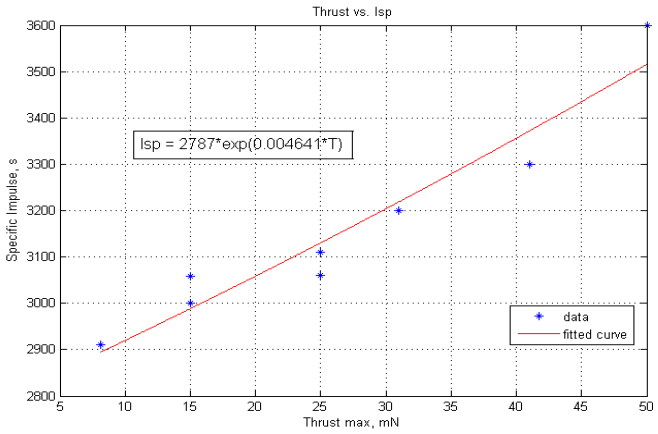

Figure 10.2: Thrust versus Specific Impulse Best Fit from the Table 2.2

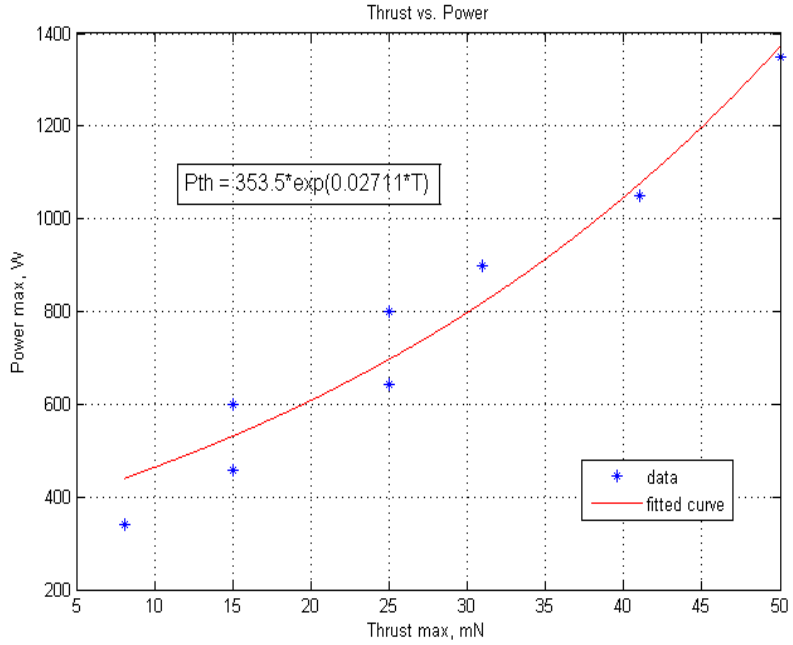

Figure 10.3: Thrust versus Thruster Power Best Fit from the Table 2.2

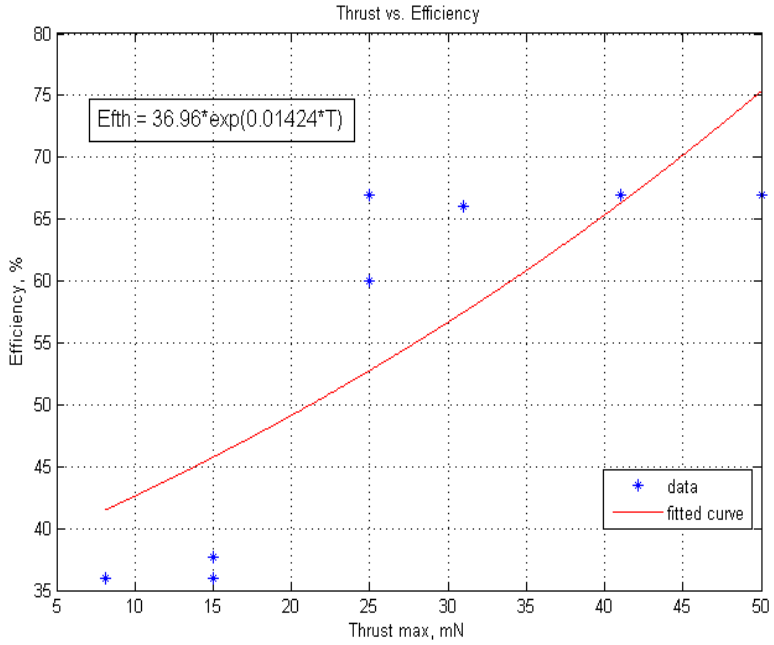

Figure 10.4: Thrust versus Thruster Efficiency from the Table 2.2

10.2 Appendix 2: HALL Thruster Best Fitting from Table 2.3

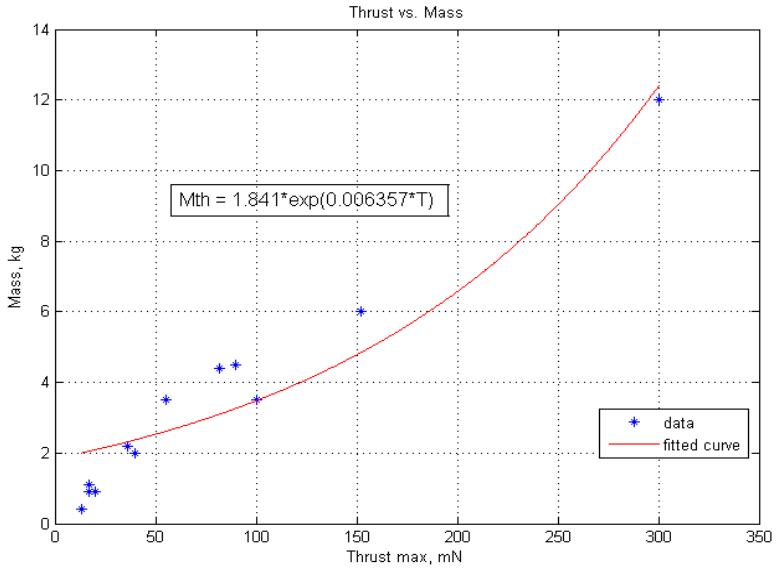

Figure 10.5: Thrust versus Thruster Mass Best Fit from the Table 2.3

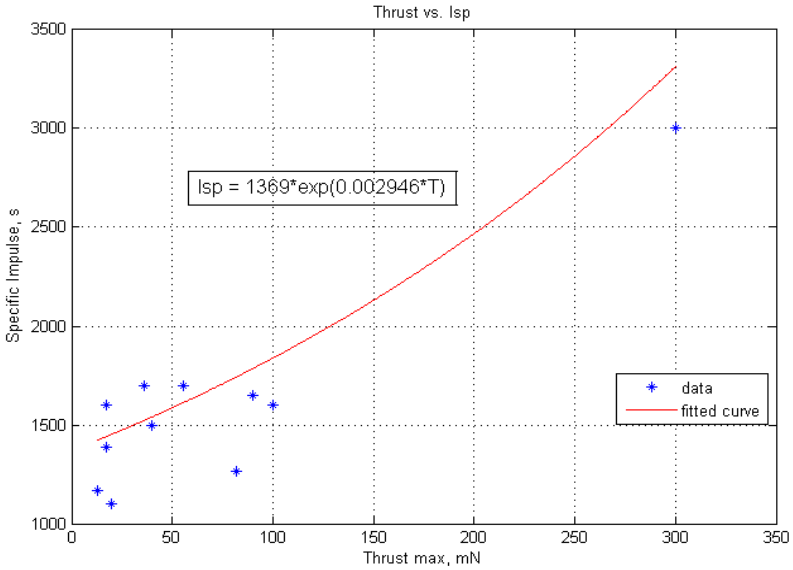

Figure 10.6: Thrust versus Specific Impulse Best Fit from the Table 2.3

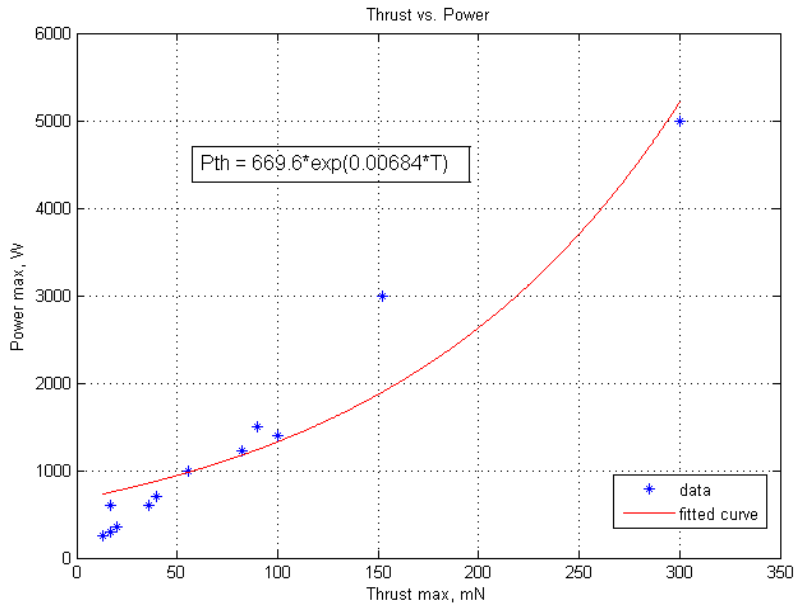

Figure 10.7: Thrust versus Thruster Power Best Fit from the Table 2.3

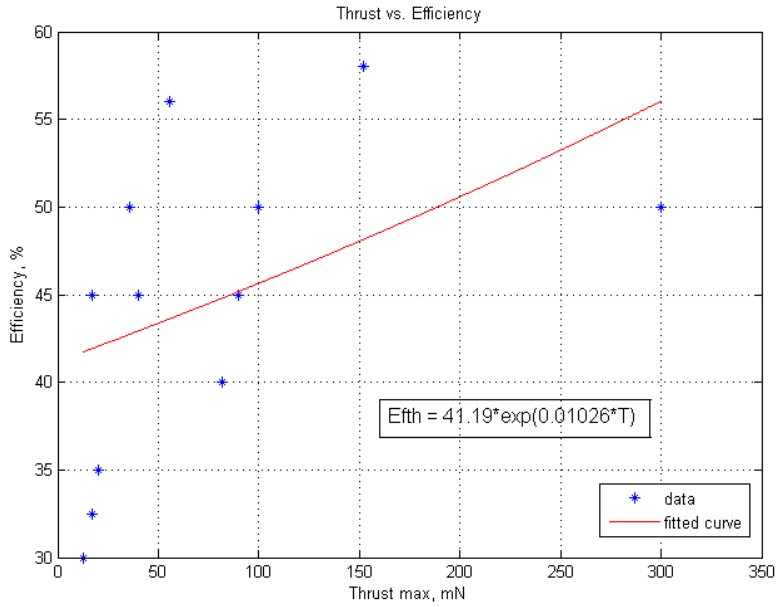

Figure 10.8: Thrust versus Thruster Efficiency Best Fit from the Table 2.3

10.3 Appendix 3: Spacecraft Data List Best Fit Equations from Tables 3.1, 3.2 and 3.3

$$P_{total} = 11.81 \times Asa^2 - 15.645 \times Asa + 339.16 \tag{10.1}$$

$$M_{propellant} = 6029.3 \times V_{tank}^2 - 550.18 \times V_{tank} + 113.01 \tag{10.2}$$

$$M_{total} = 0.0116 \times M_{propellant}^2 - 3.6073 \times M_{propellant} + 662.7561 \tag{10.3}$$

$$M_{payload} = 0.00017824 \times M_{propellant}^2 - 0.017276 \times M_{propellant} + 21.12 \tag{10.4}$$

$$A_{sa} = 1.9225 \times 10^{-7} \times Ptotal^2 + 0.002964 \times Ptotal + 4.2765 \tag{10.5}$$

$$V_{tank} = 0.012264 \times V_{SC}^2 - 0.018342 \times V_{SC} + 0.071676 \tag{10.6}$$

$$P_{total} = -1.829 \times 10^{-5} \times P_{payload}^2 + 0.046926 \times P_{payload} + 25.62 \tag{10.7}$$

BIBLIOGRAPHY

[1] *NASA LADEE Mission Press Kit*

[2] Roger Walker, *The European Student Moon Orbiter (ESMO): A lunar Mission for Education, Outreach and Science*, Acta Astronautica, 66(7-8): 1177-1188, 2010.

[3] Yvonne Clearwater, et al., *The NASA American Student Moon Orbiter (ASMO) Project*, 21st Annual AIAA/USU Conference on Small Satellites, 2007, SSC07-XI-9

[4] P. Pergola, *Small Satellite Survey Mission to the Second Earth Moon*, Advances in Space Research (COSPAR), 52(9): 1622-1633, 2013

[5] *Turkey 2023 Export Strategy and Action Plan. Retrieved from (Turkish)*

[6] Sarah Stansbury, *Low Thrust Transfer to GEO: Comparison of Electric and Chemical Propulsion*, ASEN 5050 Project, December 10, 2009

[7] *Deep Space 1, National Space Science Data Center*, NSSDC/COSPAR ID: 1998-061A

[8] H. Kuninaka et al., *Hayabusa Asteroid Explorer Powered by Ion Engines on the way to Earth*, 31st International Electric Propulsion Conference, Sept. 20-24, 2009, University of Michigan, Ann Arbor, Michigan, USA

[9] Bernard Foing et al., *Smart-1 Mission to the Moon: Technology and Science Goals*, Advances in Space Research (COSPAR), 31(11): 2323-2333, 2003

[10] Dan Goebel and Ira Katz, *Fundamentals of Electric Propulsion Ion and Hall Thrusters*, Wiley Publication, 1st Edition, 2008

[11] George Sutton and Oscar Biblarz, *Rocket Propulsion Elements*, Wiley Interscience, 7th edition, 2000

[12] T. M. Chiasson, *Modeling the Characteristics of Propulsion Systems Providing Less Than 10 N Thrust*, MSc Dissertation, Department of Aeronautics and Astronautics, Massachusetts Institute of Technology, Cambridge, MA, 2012

[13] J. Mueller, *Thruster Options for Microspacecraft: A Review and Evaluation of Existing Hardware and Emerging Technologies*, 33rd Joint Propulsion Conference and Exhibit, AIAA 1997-3058

[14] R. Killinger et al., *RITA Ion Propulsion for ARTEMIS - Lifetime Test Results*, 3rd International Conference, Oct. 10-13, 2000, Cannes, France, European Space Agency ESASP-465, 2001, pp. 433

[15] T. Misuri et al., *MEPS Programme: Development of a Low Power, Low Cost HET for Small Satellites*, Space Propulsion Conference, May 19-22, 2014, Cologne, Germany

[16] W. Tigle et al., *XIPS Ion Thruster for Small Satellite Applications*, 21st Annual AIAA/USU Conference on Small Satellites, 2007, SSC07-III-11

[17] C. H. Edwards et al., *The T5 Ion Propulsion Assembly for Drag Compensation on GOCE*, 2nd International GOCE User Workshop, GOCE The Geoid and Oceanography, ESA-ESRIN, March 8-10, 2004, Italy, ESA SP-569, June 2004

[18] E. Bourguignon et al., *Power Processing Unit Activities at Thales Alenia Space Belgium (ETCA)*, 33rd International Electric Propulsion Conference, Oct. 6-10, 2013, The George Washington University, Washington DC, USA

[19] *Electric Propulsion, 30 cm NSTAR Power Processor*, L-3 Electron Technologies Inc. Product Lines

[20] H. De Clercq et al., *High Power Processing Unit for Stationary Plasma Thruster*, Spacecraft Propulsion, 3rd International Conference, Oct. 10-13, 2000, Cannes, France, European Space Agency ESASP-465, 2001., pp. 601

[21] S. D. Clark et al., *BepiColombo Electric Propulsion Thruster and High Power Electronics Coupling Test Performances*, 33rd International Electric Propulsion Conference, Oct. 6-10, 2013, The George Washington University, Washington DC, USA

[22] H. Osuka et al., *Development Status of Power Procession Unit for 200mN-class Hall Thruster*, 29th International Electric Propulsion Conference, Oct.6-Nov.4, 2006, Princeton University, USA

[23] D. Fiehler et al., *Electric Propulsion System Modeling for the Proposed Prometheus 1 Mission*, 41st Joint Propulsion Conference and Exhibit, AIAA, July 10-13, 2005, Tuscon, Arizona, NASA/TM2005-213892

[24] Dr. David R. Williams, *Clementine Project Information*, National Space Science Data Center

[25] D. Rayman et al., *Dawn: A Mission in Development for Exploration of Main Belt Asteroids Vesta and Ceres*, Acta Astronautica, 58(11): 605-616, June 2006

[26] *NASA Grail Mission Press Kit*, August 2011

[27] H. Kuninaka et al., *Hayabusa 2 Update*, 10th Meeting of the Small Bodies Assessment Group, Jan. 8-9, 2014, Washington DC, USA

[28] R. C. Elphic and C. T. Russell, *The Lunar Atmosphere and Dust Environment Explorer (LADEE)*, Springer, New York, 2015

[29] *Lunar Crater Observation and Sensing Satellite, LCROSS, Search for Water*, Lunar Prospector Mission Project Description, NASA Mission Page

[30] *Mars Odeyssey 2001*, NASA JPL MARS Odeyssey Mission Page

[31] Dr. David R. Williams, *Near Shoemaker*, National Space Science Data Center

[32] Dr. David R. Williams, *Stardust Flight System Description*, NASA JPL

[33] J. Kechichian, *Reformulation of Edelbaums Low-Thrust Transfer Problem Using Optimal Control Theory*, Journal of Guidance, Control and Dynamics, AIAA, 20(5): 988-994, 1997

[34] V. Chobotov *Orbital Mechanics*, Chapter 14, 3rd Edition, AIAA Education Series, New York, 2002

[35] T. M. Edelbaum, *Propulsion Requirements for Controllable Satellites*, ARS Journal, 31(8): 1079-1089, 1961

[36] R. P. Welle, *Propellant Storage Considerations for Electric Propulsion*, 22nd IEPC, Oct. 1991, Viareggio, Italy, 91-107

[37] J. R. Wertz, D. F. Everett and J. J. Puschell, *Space Mission Engineering: The New SMAD*, Microcosm Press, 1st Edition, July 2011

[38] S. Bailey and R. Rafaelle, *Handbook of Photovoltaics Science and Engineering*, Chapter 10, Space Solar Cells and Arrays, edited by A. Luque and S. Hegedus, John Wiley and Sons Ltd, 2003

[39] *Turkish General Directorate of Aeronautics and Astronautics Technologies, Space Regulation Working Group Report*

[40] *TAI Presentation on Small Satellites*

[41] Ozan Kara and Arif Karabeyoglu, *Electric Propulsion Optimization of Microsatellite Moon Missions Preliminary Design Application on CubeSats and Turkish Small Satellite Field*, International Astronautical Congress, 2014, Toronto, Canada

[42] Cagri Kilic and A. Rustem Aslan, *Mission analysis of a 2U CubeSat, BeEagleSat*, 7th International Conference on Recent Advances in Space Technologies 2015, IEEE, pp. 835-838

[43] *SSM Space Launch System Project*, July 2015

[44] *Gumush Aerospace and Defense Ltd.*

[45] *The Space Economy at a Glance (2014)*, OECD, 2014

[46] Cagri Kilic et al., *Deployment Strategy Study of QB50 Network of CubeSats*, 6th International Conference on Recent Advances in Space Technologies 2013, IEEE

[47] *Vision 2023 Project, Security, Aeronautics and Space Industry Panel Report*, TUBITAK, Ankara

[48] *Turkey 2023 Export Strategy and Action Plan*, SASAD

[49] Ozan Kara, *Small Satellite Architecture Optimization: Electric Propulsion Moon Imaging Mission*, AIAA SPACE 2015, Pasadena, California

VITA

Ozan Kara was born in Bakırköy, İstanbul, Turkey on June 16th, 1990. He graduated from Burhaniye High School, Balıkesir in 2008. He received his B.Sc. degree from Istanbul Technical University, Astronautical Engineering. He enrolled KOC University M.Sc. program at the Department of Mechanical Engineering in 2014. During his M.Sc. degree he worked as a teaching and research assistant at KOC University. He has published 10 papers at the International Astronautical Congress and AIAA Space conferences related to system-level optimization of lunar mission, gamification technique in Mars Mission Design, CubeSat Lunar Mission, CubeSat Swarms Communication and Navigation and Workforce Development in the space sector. He has been selected as first Young Professional Delegate of Turkey by the IAC YP Workshop Organizing Committee in 2012. He is the member of AIAA Systems Engineering Technical Committee, AIAA Young Professional Committee, and Space Generation Advisory Council.